

1 **Recent tectonic reorganization of the Nubia-Eurasia convergent**
2 **boundary heading for the closure of the western Mediterranean**

3

4 Andrea Billi ^{1*}, Claudio Faccenna ^{1,2}, Olivier Bellier ³, Liliana Minelli ⁴, Giancarlo Neri ^{4,5}, Claudia
5 Piromallo ⁴, Debora Presti ^{2,5}, Davide Scrocca ¹, and Enrico Serpelloni ⁶

6

7 ¹ *Istituto di Geologia Ambientale e Geoingegneria, CNR, Rome, Italy.*

8 ² *Dipartimento di Scienze Geologiche, Università Roma Tre, Rome, Italy;*

9 ³ *UMR CEREGE - 6635, CNRS, Université Paul Cézanne, Aix-Marseille Université, IRD, Collège de France, Europôle*
10 *de l'Arbois, BP. 80, 13545 Aix-en-Provence, France.*

11 ⁴ *Istituto Nazionale di Geofisica e Vulcanologia, Rome, Italy;*

12 ⁵ *Dipartimento di Scienze della Terra, Università di Messina, Messina, Italy;*

13 ⁶ *Istituto Nazionale di Geofisica e Vulcanologia, Centro Nazionale Terremoti, Bologna, Italy;*

14 * *Corresponding author: Istituto di Geologia Ambientale e Geoingegneria (IGAG), CNR, Area della Ricerca Roma 1,*
15 *Via Salaria km 29,300, Monterotondo, 00016, Roma, Italy, Tel. +39 06-90672732, email: andrea.billi@cnr.it*

16 **Abstract:** In the western Mediterranean area, after a long period (late Paleogene-Neogene) of
17 Nubian (W-Africa) northward subduction beneath Eurasia, subduction is almost ceased as well as
18 convergence accommodation in the subduction zone. With the progression of Nubia-Eurasia
19 convergence, a tectonic reorganization is therefore necessary to accommodate future contraction.
20 Previously-published tectonic, seismological, geodetic, tomographic, and seismic reflection data
21 (integrated by some new GPS velocity data) are reviewed to understand the reorganization of the
22 convergent boundary in the western Mediterranean. Between northern Morocco, to the west, and
23 northern Sicily, to the east, contractional deformation has shifted from the former subduction zone
24 to the margins of the two backarc oceanic basins (Algerian-Liguro-Provençal and Tyrrhenian
25 basins) and it is now mainly active in the south-Tyrrhenian (northern Sicily), northern Liguro-
26 Provençal, Algerian, and Alboran (partly) margins. Onset of compression and basin inversion has
27 propagated in a scissor-like manner from the Alboran (c. 8 Ma) to the Tyrrhenian (younger than c. 2
28 Ma) basins following a similar propagation of the subduction cessation, i.e., older to the west and
29 younger to the east. It follows that basin inversion is rather advanced in the Algerian margin, where
30 a new southward subduction seems to be in its very infant stage, while it has still to properly start in
31 the Tyrrhenian margin, where contraction has resumed at the rear of the fold-thrust belt and may
32 soon invert the Marsili oceanic basin. Part of the contractional deformation may have shifted toward
33 the north in the Liguro-Provençal basin possibly because of its weak rheological properties
34 compared with those ones of the area between Tunisia and Sardinia, where no oceanic crust occurs
35 and seismic deformation is absent or limited. The tectonic reorganization of the Nubia-Eurasia
36 boundary in the study area is still strongly controlled by the inherited tectonic fabric and rheological
37 attributes, which are strongly heterogeneous along the boundary. These features prevent, at present,
38 the development of long and continuous thrust faults. In an extreme and approximate synthesis, the
39 evolution of the western Mediterranean is inferred as being similar to a Wilson Cycle (at a small
40 scale) in the following main steps: (1) northward Nubian subduction with Mediterranean backarc
41 extension (since ~35 Ma); (2) progressive cessation, from west to east, of Nubian main subduction

42 (since ~15 Ma); (3) progressive onset of compression, from west to east, in the former backarc
43 domain and consequent basin inversion (since ~8-10 Ma); (4) possible future subduction of former
44 backarc basins.

45

46 **Key words:** western Mediterranean, convergent boundary, tectonic reorganization, subduction,
47 backarc basin, basin inversion.

48

49

50 **Réorganisation tectonique récente du domaine de convergence de plaque Nubie-Eurasie en**
51 **Méditerranée occidentale.**

52

53 **Résumé:** En Méditerranée occidentale, après une longue période (Paléogène supérieur et Néogène)
54 de subduction de la plaque nubienne sous l'Eurasie, la subduction s'arrête et la convergence doit
55 alors être accommodée par d'autres processus géodynamiques impliquant une réorganisation
56 tectonique de la méditerranée occidentale.

57 Une synthèse des données tectoniques, sismologiques, géodésiques, tomographiques, et de
58 sismique réflexion complétée par de nouvelles mesures géodésiques, nous permet de proposer un
59 modèle de cette réorganisation tectonique intégré à l'échelle de la Méditerranée occidentale. Entre le
60 Nord du Maroc et le Nord de la Sicile, la déformation compressive résultant de la convergence s'est
61 déplacée de la zone de subduction vers les marges des bassins océaniques d'arrière arc, que sont les
62 bassins Algéro-Liguro-Provençal et Tyrrhénien. Les marges Tyrrhénienne (Nord de la Sicile),
63 Liguro Provençale (SE de la France), Algérienne et de l'Alboran sont par ailleurs toujours actives.
64 La compression, ainsi que l'inversion tectonique associée, se sont propagées, du bassin d'Alboran
65 (c. 8 Ma) vers le domaine Tyrrhénien (< c.2Ma), parallèlement à la rupture du slab due à l'arrêt de
66 la subduction. Ensuite l'inversion s'est propagée vers la marge algérienne soumise à une subduction
67 embryonnaire vers le Sud. La compression le long de la marge Tyrrhénienne semble alors
68 accommodée en arrière par une ceinture de plis et chevauchements actifs. Une partie de la

69 compression résultant de la convergence s'est déplacée vers le Nord, sur la marge Liguro-
70 Provençale, du fait de conditions rhéologiques plus favorables que dans le domaine entre la Tunisie
71 et la Sardaigne où il n'y a pas de croûte océanique. Ce domaine est d'ailleurs caractérisé par une
72 très faible activité sismique par rapport aux autres domaines frontaliers des plaques Nubie et
73 Eurasie.

74 Globalement, la réorganisation géodynamique aux limites de plaques Nubie – Eurasie est fortement
75 contrôlée par l'héritage tectonique et les conditions rhéologiques qui varient notablement, et qui,
76 d'autre part, ne sont pas cylindriques le long de cette zone de frontière. Ces conditions aux limites
77 empêchent le développement de systèmes de chevauchement longs et continus.

78 En résumé, l'évolution finie-cénozoïque suit un cycle de Wilson avec quatre étapes majeures: 1- une
79 subduction vers le nord de la plaque nubienne qui produit une extension «classique» d'arrière arc
80 depuis 35 Ma; 2- à partir de 15 Ma, un arrêt de la subduction qui se propage de l'Ouest vers l'Est, le
81 long de la frontière de plaque; 3- à environ 8-10 Ma, on assiste à la mise en place d'une déformation
82 compressive, de l'Ouest vers l'Est, en domaine d'arrière arc qui induit une inversion tectonique; 4-
83 enfin, la possibilité de mise en place de nouvelles zones de subduction dans ces zones arrière arc.

84

85 **Mots clefs:** Méditerranée occidentale, frontière de plaque en convergence, réorganisation
86 tectonique, subduction, bassin d'arrière arc, inversion tectonique.

87 **1. INTRODUCTION**

88 Both recent and old suture zones between continental plates usually consist of a complex
89 juxtaposition of highly-deformed tectonic slices deriving from pristine paleogeographic and
90 geodynamic domains as diverse as oceanic basins, sedimentary prisms, subduction complexes,
91 volcanic arcs, seamounts, isolated continental blocks, and backarc basins [e.g., Cloetingh *et al.*,
92 1982; Burg and Chen, 1984; Cloos, 1993; van der Voo *et al.*, 1999; Murphy and Yin, 2003]. In
93 several cases, evidence of multiple subduction events either contemporary or succeeding with even
94 opposite polarities are documented or hypothesized in tectonic sutures [e.g., Teng *et al.*, 2000;
95 Michard *et al.*, 2002; Tyson *et al.*, 2002; White *et al.*, 2002; Kapp *et al.*, 2003; Doglioni *et al.*,
96 2007; Regard *et al.*, 2008]. The juxtaposition of heterogeneous tectonic slices shows that the
97 process occurring along destructive tectonic boundaries and anticipating the continental collision or
98 the final suture often does not simply consist of an oceanic lithosphere steadily and cylindrically
99 subducting beneath a continental one. Large and deep backarc oceanic basins may, for instance,
100 develop during long periods of oceanic subduction. With the progression of plate convergence on
101 the way to tectonic suture, these extensional structures may be inverted and even closed through the
102 subduction of the oceanic lithosphere in the former backarc domains [e.g., Escayola *et al.*, 2007;
103 Vignaroli, Faccenna *et al.*, 2008].

104 One ideal region to study the tectonic processes anticipating the final suture between
105 continents is the Mediterranean region (Fig. 1), where the Nubian (i.e., the African plate to the west
106 of the eastern rift) and Eurasian plates meet and interact within the general framework of active
107 convergence [Dercourt *et al.*, 1986; Dewey *et al.*, 1989; Ricou *et al.*, 1986; Doglioni, 1991;
108 Cloetingh and Kooi, 1992; Jolivet and Faccenna, 2000; Jolivet *et al.*, 2003; Rosenbaum *et al.*, 2002;
109 Stich *et al.*, 2003; Allen *et al.*, 2004; Nocquet and Calais, 2004; Nocquet *et al.*, 2006; Fernández-
110 Ibáñez *et al.*, 2007; Mauffret, 2007; Serpelloni *et al.*, 2007; D'Agostino *et al.*, 2008; Zitellini *et al.*,
111 2009; Carminati *et al.*, 2010; Lustrino *et al.*, 2011]. The western Mediterranean (i.e., from Calabria,
112 southern Italy, to Algeria and Gibraltar), in particular, is a tectonically complex area where two

113 small oceanic basins (Tyrrhenian and Liguro-Provençal backarc basins) occur along the Nubia-
114 Eurasia convergent margin and are separated by the Corsica-Sardinia rigid continental block
115 [Doglioni *et al.*, 1997; Gueguen *et al.*, 1997; Jolivet and Faccenna, 2000; Faccenna *et al.*, 2001,
116 2002; Mascle *et al.*, 2004; Jolivet *et al.*, 2008]. Such a complex setting imposes a segmentation and
117 reorganization of the convergent boundary as well as a complex (i.e., non-cylindrical) distribution
118 of the zones accommodating the contractional deformation. The particular and favorable tectonic
119 setting of the western Mediterranean may allow researchers to capture some snapshots of the very
120 early processes of tectonic inversion eventually leading to the closure of backarc basins and final
121 suture between continents. Assuming that the closure of the western Mediterranean basin will
122 occur, at least in part, through subduction of the two backarc oceanic basins (Tyrrhenian and
123 Liguro-Provençal), studying and monitoring them may provide insights into subduction inception
124 [e.g., Cloetingh *et al.*, 1982; Souriau, 1984; Toth and Gurnis, 1998; Faccenna *et al.*, 1999; House *et*
125 *al.*, 2002; Strzeczynski *et al.*, 2010].

126 In this paper, we address the present and recent tectonic reorganization along the Nubia-
127 Eurasia convergent boundary in the central-western Mediterranean. To do so, we review previously-
128 published datasets (integrated by some new GPS velocity data) constraining the present tectonic
129 architecture and regime. We analyze, in particular, structural, geodetic, seismological, seismic
130 reflection, and tomographic data. Based on these data, we discuss possible tectonic models
131 explaining the reported datasets and eventually provide some implications for future tectonic
132 scenarios of the studied tectonic boundary. As most strong earthquakes and related destructive
133 tsunamis are generated at convergent margins and subduction zones [McCaffrey, 2008], this paper
134 bears implications into earthquake and tsunami hazard in the Mediterranean even though this
135 subject is beyond our aims.

136

137

138

139 2. EVOLUTION OF THE WESTERN MEDITERRANEAN SUBDUCTION ZONE

140 The late Paleogene-Neogene tectonic evolution of the western Mediterranean has been
141 drawn in a series of studies based on geological, geophysical, and geochemical constraints
142 supported, in some cases, by numerical and physical modeling [Malinverno and Ryan, 1986;
143 Kastens *et al.*, 1988; Dewey *et al.*, 1989; Doglioni, 1991; Patacca *et al.*, 1992; Carminati *et al.*,
144 1998; Carminati, Wortel, Spakman, and Sabadini 1998; Jolivet and Faccenna, 2000; Faccenna *et*
145 *al.*, 2004, 2005; Rosenbaum and Lister, 2004; Pepe *et al.*, 2005, 2010; Minelli and Faccenna, 2010].
146 Most of these studies use a slab retreat model [e.g., Malinverno and Ryan, 1986; Royden, 1993;
147 Lallemand *et al.*, 2008; Jolivet *et al.*, 2009] to explain the present tectonic setting of the study area
148 that includes fold-thrust belts and backarc basins along the Nubia-Eurasia convergent boundary,
149 which is also known as the western Mediterranean subduction zone [Faccenna *et al.*, 2004]. Three
150 main tectonic domains can be recognized along this zone: the inner and outer orogenic domains,
151 and the extensional backarc domain (Fig. 1).

152 The inner orogenic domain mostly consists of stacked slices of continental crystalline
153 Variscan basement with its metasedimentary cover. Ophiolitic units are exposed in Calabria and
154 northern Apennines, whereas the continental crystalline and metasedimentary formations are
155 extensively exposed in the northern Apennines, Calabria, Kabylie, and Rif-Betic belts [Dercourt *et*
156 *al.*, 1986; Monié *et al.*, 1988; Platt *et al.*, 1998; Caby *et al.*, 2001; Vignaroli *et al.*, 2009; Rossetti *et*
157 *al.*, 2001, 2004, 2010].

158 The outer orogenic domain is overthrust by the inner domain and is mostly constituted by a
159 stack of Meso-Cenozoic thrust sheets of sedimentary rocks deriving from the deformation of the
160 African, Iberian, and Adriatic continental margins. This domain mostly developed during Neogene
161 time with lateral heterogeneities in the geometry of structures and direction of tectonic transport
162 (i.e., see the Calabria and Gibraltar arcs; Roure *et al.*, [1991]; Outtami *et al.*, [1995]; Gomez *et al.*,
163 [1998]; Frizon de Lamotte *et al.*, [2000]; Thomas *et al.*, [2010]).

164 The extensional backarc domain includes two main triangular backarc basins partly flooded
165 by oceanic crust: the Tyrrhenian basin, to the east, and the larger and older Liguro-Provençal basin,
166 to the west, which elongates toward Gibraltar, where the Algerian and Alboran basins occur
167 [Kastens *et al.*, 1988; Kastens and Mascle, 1990; Sartori, 1990; Gorini *et al.*, 1994; Faccenna *et al.*,
168 1997]. The Tyrrhenian and Liguro-Provençal basins are separated by the Corsica-Sardinia
169 continental block [Mascle *et al.*, 2004].

170 The above-mentioned structures are obviously correlated with the Moho depth in the
171 western Mediterranean area [Tesauro *et al.*, 2008; Fig. 1b]. The Moho is shallow in the Tyrrhenian
172 and Liguro-Provençal basins up to a minimum of only about 5 km and tends to deepen toward the
173 surrounding continental areas and fold-thrust belts (Alps, Apennines, Betics, Pyrenees, and Rif-
174 Atlas) up to a maximum of about 55 km in the northeastern Alps. In several cases, the backarc
175 basins developed in crustal areas thickened during previous phases of mountain belt building.
176 Afterward, backarc extension led to the exhumation of high-pressure metamorphic and plutonic
177 rocks that are well exposed, for instance, in Corsica, and peri-Tyrrhenian, Alboran, and Aegean
178 areas [Jolivet *et al.*, 1990; Gautier and Brun, 1994; Platt *et al.*, 1998; Jolivet and Faccenna, 2000;
179 Rossetti *et al.*, 2001, 2004].

180 Fig. 2 shows a schematic evolutionary model of the western Mediterranean subduction zone
181 since about 35 Ma [Rehault *et al.*, 1984; Carminati *et al.*, 1998; Frizon de Lamotte *et al.*, 2000;
182 Faccenna *et al.*, 2004]. This model is useful to understand the formation of backarc basins and their
183 recent inversion.

184 At about 35 Ma, the subduction zone ran almost continuously from Gibraltar to Liguria (i.e.,
185 in a present-day geographic perspective) possibly along a NE-SW direction. This boundary was
186 consuming a Mesozoic ocean that subducted toward the northwest with a decreasing velocity
187 toward the west (Gibraltar), where continental collision had almost occurred.

188 At about 30 Ma, backarc extension started in the northern part of the Liguro-Provençal basin
189 and then propagated toward the south in the Valencian and Alboran basin. This process was

190 accompanied by widespread calc-alkaline volcanism in regions such as Sardinia, Valencian, and
191 Alboran, and was induced by the slab retrograde fast motion.

192 Between about 23 and 15 Ma the opening of the Liguro-Provençal basin was mostly
193 accomplished, but extension was still active in the Alboran basin at about 15 Ma. At that time, in
194 fact, the western portion of the slab broke off and the subduction zone became discontinuous in the
195 Mellilla-Oranie region, where NE-SW left-lateral tectonics occurred (Table 1). This process left the
196 western portion of the slab free to rapidly retreat and drive backarc extension in the Alboran region.
197 Also at this stage, the entire subduction zone was characterized by the presence of calc-alkaline
198 volcanism, whose melt was possibly generated through the crustal contamination of a mantle
199 metasomatized melt [e.g., Fourcade *et al.*, 2001; Coulon *et al.*, 2002].

200 Afterward, extension shifted in the Algerian basin and then in the Tyrrhenian region, where
201 synrift sedimentation started at about 10-12 Ma [Kastens and Mascle, 1990], and basaltic volcanism
202 occurred at 4-5 Ma in the Vavilov basin and at 2 Ma in the Marsili basin [Sartori, 1990; Nicolosi *et*
203 *al.*, 2006]. Also in this case, episodes of intense backarc extension are possibly related with
204 episodes of lateral slab tearing (Table 1) and associated subduction zone segmentation that
205 facilitated the retrograde motion of a progressively narrower slab in the eastern sector of the
206 subduction zone. In particular, the Nefza and Mogodos, Tunisia, (Na)-alkaline basalts (circa 8-6
207 Ma) are interpreted as due to the lateral segmentation of the slab and consequent mantle return
208 flows around the ruptured slab, which was then free to retreat toward the southeast in the
209 Tyrrhenian region. Analogously, the sodic-alkaline magmatism of Ustica and Prometeo in the
210 south-western Tyrrhenian probably marks a further episode of slab breakoff and enhanced retreat of
211 the subduction zone during Messinian-Pliocene time (circa 4-5 Ma) [Faccenna *et al.*, 2005].

212 In Fig. 2, backarc compression and inversion start, from the west, prior than 5 Ma and then
213 propagate toward the east [Wortel and Spakman, 2000; Faccenna *et al.*, 2004] (Table 1). This
214 evolution is the main subject of this paper and it is addressed in the following sections.

215

216 3. FROM SUBDUCTION TO BACKARC COMPRESSION AND INVERSION

217 In the western Mediterranean area, seismological data (see next section) and other
218 geophysical and geological evidence show that some strands of the backarc basin margins have
219 recently undergone and are presently undergoing compressional tectonics [e.g., Serpelloni *et al.*,
220 2007]. This tectonic regime, in particular, is active, from west to east, along the east-Alboran,
221 Algerian, and south-Tyrrhenian margins. Seismicity between Tunisia, northwestern Sicily, and
222 Sardinia is weaker and less frequent than off Algeria and northern Sicily, whereas on the opposite
223 side of the western Mediterranean (toward the north), in the northern Liguro-Provençal margin, in
224 Provence (France), and in Liguria (Italy), a seismicity slightly stronger than that of the area between
225 Tunisia and Sardinia occurs. Also a portion of southern Spain (the northeastern margin of the
226 Alboran basin) is undergoing contraction as attested by compressional earthquakes, geological-
227 geophysical evidence, and GPS data [Fernández-Ibáñez *et al.*, 2007; Serpelloni *et al.*, 2007].

228

229 **Alboran margin** - The present tectonic setting of the Alboran Sea area (Fig. 1) is the result
230 of a complex orogenic evolution occurred mostly during Cenozoic time within the framework of
231 Eurasian-Nubian plate convergence [Michard *et al.*, 2002; Platt *et al.*, 2003; Duggen *et al.*, 2004,
232 2005 Rossetti *et al.*, 2010]. The area presently includes the Rif and Betic fold-thrust belts in
233 northern Morocco and southern Spain, respectively, and the Gibraltar Arc that connects these
234 structures in the Atlantic area (Gulf of Cadiz), where an eastward narrow subducting slab is
235 supposed to be still active and seismogenic [Gutscher *et al.*, 2002, 2009]. The inner (Mediterranean)
236 sector of the curved fold-thrust belt includes the Alboran narrow basin that is articulated in sub-
237 basins and troughs, and is characterized by a thinned transitional crust (circa 10-12 km in the
238 eastern sector) compared with the surrounding belt (up to circa 30-35 km) [Torne *et al.*, 2000].
239 Extension in the Alboran basin developed mostly during Burdigalian-Langhian times [Bourgeois *et al.*
240 *et al.*, 1992; Mauffret *et al.*, 1992] possibly because of slab rollback [Royden, 1993; Lonergan and
241 White, 1997; Faccenna *et al.*, 2004].

242 Compression resumed in the Alboran area since about 8 Ma (Table 1), producing reverse
243 and strike-slip faulting and related folding, which have involved, since then, the entire basin (i.e.,
244 diffuse deformation) and not only its margins [Bourgois *et al.*, 1992; Campos *et al.*, 1992; Comas *et*
245 *al.*, 1992, 1999; Mauffret *et al.*, 1992; Morel and Meghraoui, 1996]. NNW-SSE compression
246 resumed at the end of Tortonian time (c. 8 Ma) also along the northern margin of the Alboran Basin
247 (e.g., Granada basin, southern Spain) after a period, during Miocene time, of extension and
248 exhumation of metamorphic complexes [Martínez- Martínez *et al.*, 2002; Rodríguez-Fernández and
249 Sanz de Galdeano, 2006]. Toward the west, off southwestern Portugal, the Goringe Bank
250 developed by NW-verging subcrustal thrusting at c. 8 Ma or slightly earlier (10.5 Ma) [Jiménez-
251 Munt *et al.*, 2010].

252 The present tectonic activity in the Alboran and surrounding areas is proved by instrumental
253 and historical earthquakes [Bufoin *et al.*, 1995, 2004; Morel and Meghraoui, 1996; López Casado *et*
254 *al.*, 2001; Gràcia *et al.*, 2006]. Instrumental earthquakes are predominantly low magnitude ($M < 5$),
255 but $M > 5$ earthquakes occurred both in historical and instrumental times. For instance, the Al
256 Hoceima area (located on the Moroccan coast in front of the central Alboran Sea) experienced
257 several destructive earthquakes. Significant events or swarms dated 1522, 1624, 1791, and 1800-
258 1802 have been reported by El Mrabet [2005]. Afterward, a M 5.9 earthquake was generated in this
259 area by a left-lateral strike-slip buried fault [Calvert *et al.*, 1997], and, eventually, the strong (M 6.3)
260 Al Hoceima earthquake occurred on 24 February 2004 generated by a NNE-striking, right-lateral,
261 strike-slip fault [Stich *et al.*, 2005]. Earthquakes in the Alboran basin occurred in response to a
262 complex stress regime resulting from the general NW-SE Eurasia-Nubia compression combined
263 with local stress sources, which induce anticlockwise rotation of the maximum compression up to
264 almost 80° [Fernández-Ibáñez *et al.*, 2007]. The resulting tectonic regime is, on average,
265 compressive in the eastern portion of the Alboran basin and off Gibraltar in the Atlantic Ocean, and
266 transtensional in the central-western portion of the Alboran basin [Stich *et al.*, 2006; Serpelloni *et*
267 *al.*, 2007].

268

269 **Algerian margin** - The Algerian basin is located to the east of the Alboran basin, between
270 the Sardinia and Balearic blocks (Fig. 1). The crust thins from about 7 km in the Alboran basin to
271 about 4 km in the Algerian basin and changes its nature from transitional to oceanic [Comas *et al.*,
272 1997; Catalano *et al.*, 2000; Tesauro *et al.*, 2008].

273 Northern Algeria includes the Atlas-Tell fold-thrust belt, which developed during Cenozoic
274 times in response to the collision between the Kabylia block (European affinity) and the Nubian
275 plate. Along this boundary, the Tethyan oceanic lithosphere subducted toward the north since
276 Eocene or Oligocene times [Rosenbaum *et al.*, 2002] with a significant dextral oblique component
277 [Saadallah *et al.*, 1996]. Because of slab rollback [Jolivet and Faccenna, 2000], the Algerian basin
278 formed in the backarc area [Roca *et al.*, 2004] with stretching starting possibly since late Oligocene-
279 early Miocene times [Dewey *et al.*, 1989; Rosenbaum and Lister, 2004]. Ductile extension dated at
280 c. 25 Ma in the Grand Kabylie [Monié *et al.*, 1984; Saadallah and Caby, 1996] supports the age of
281 stretching onset. The opening of the Algerian basin involved the formation of oceanic crust as
282 recently shown by wide-angle seismic surveys [Pesquer *et al.*, 2008]. Magnetic anomalies of the
283 Algerian basin suggest compartmentalization of this basin and related strike-slip faulting during its
284 growth [Maillard and Mauffret 1999; Schettino and Turco, 2006].

285 With continental collision and subsequent slab breakoff (Table 1), spreading of the Algerian
286 basin ceased during Burdigalian-Langhian time (c. 15 Ma) as also supported by the chemical
287 change of volcanism along the Algerian margin [Maury *et al.*, 2000]. Although extensional
288 displacements may have persisted until even 6 Ma, main extension in the Algerian basin endured
289 until about 8 Ma when the Tyrrhenian basin formation had already started [Mauffret *et al.*, 2004].
290 Compressional inversion of the Algerian basin started afterward during late Miocene time (c. 5-7
291 Ma) and then progressed during Pliocene-Quaternary times [Auzende *et al.*, 1975; Meghraoui *et al.*,
292 1986; Déverchère *et al.*, 2005; Domzig *et al.*, 2006; Mauffret, 2007] when extension and oceanic
293 crust emplacement were active toward the east in the Tyrrhenian basin (Table 1). In particular, N-

294 dipping S-verging reverse structures developed or were reactivated in the onshore portion of the
295 Algerian margin, whereas S-dipping N-verging faults developed mainly as newly-originated
296 structures at the transition between continental and oceanic domains off Algeria [Déverchère *et al.*,
297 2005; Domzig *et al.*, 2006; Mauffret, 2007; Yelles *et al.*, 2009; Kherroubi *et al.*, 2009], thus
298 suggesting a southward subduction inception of the Algerian basin [Strzeczynski *et al.*, 2010]. The
299 active margin off Algeria is, however, still poorly organized (laterally) and consists of several fault
300 strands, which are unconnected or connected through perpendicular or oblique tear faults. This
301 pattern is at least in part inherited from pre-existing structures [Strzeczynski *et al.*, 2010]. A similar
302 pattern, although with opposite vergence and dip of reverse faults, and a younger age, is observed
303 along the south-Tyrrhenian margin [Pepe *et al.*, 2005; Billi, Presti *et al.*, 2007].

304 Unlike the Alboran basin, compressional structures and inversion tectonics of the Algerian
305 margin are rather concentrated as also shown by reflection seismics. Figs. 3(a) and 3(b) show two
306 high-resolution seismic profiles acquired across the Algerian margin [Déverchère *et al.*, 2005;
307 Domzig *et al.*, 2006; Kherroubi *et al.*, 2009], displaying some evidence or clues of basin margin
308 inversion. Fig. 3(a), in particular, shows a profile from the eastern Algeria (Annaba area), running
309 from the continental margin to the deep basin along a track perpendicular to the main structures of
310 the area. The profile interpretation includes S-dipping, N-verging reverse faults at the foot of the
311 continental platform. Although no historical earthquakes are reported for this area, these fault
312 segments could have been responsible for large past events. Moreover, the profile displays a well
313 stratified Plio-Quaternary unit on top of Messinian unit (UE) folded in asymmetrical anticlines with
314 gently-dipping, relatively-flat, long, landward backlimbs, and steeper and shorter seaward limbs.
315 The upper part of the Plio-Quaternary unit shows growth strata onlapping the landward limb of
316 folds, thus depicting an active or recently-active fault-related fold system [Kherroubi *et al.*, 2009].

317 Fig. 3(b) shows a high-resolution seismic profile acquired during the Maradja Cruise (2003)
318 across the lower slope and deep basin off Algiers [Déverchère *et al.*, 2005; Domzig *et al.*, 2006].
319 The profile shows a series of N-verging fault-propagation folds characterized by slope breaks and

320 curved scarps. In the profile, the presence of a wedged piggyback basin with active growth strata
321 developed above a thrust ramp rooted below the Messinian salt-layer is evident. The tilting of strata
322 in the basin begun during Pliocene time and is still active. Below the basinal deposits, typical salt
323 deformations are present (see S in Fig 3b).

324 The compressional tectonics presently acting along the Algerian margin is also proved by
325 strong compressional earthquakes recorded in recent (instrumental) and historical times. These
326 earthquakes are consistent with other evidence such as GPS data (see next sections and Serpelloni *et*
327 *al.*, 2007). Based on historical, instrumental, and tectonic evidence, the maximum potential
328 magnitude attributed to earthquakes in the Algerian margin is c. 7.3 [Rothé, 1950; Benouar, 2004;
329 Strzeczynski *et al.*, 2010]. Three recent moderate-to-strong earthquakes, i.e., the 1980, M 7.1 El
330 Asnam, the 1989, M 5.7 Tipaza, and the 2003, M 6.9 Boumerdès earthquakes, are representative of
331 the present compressional tectonics of the Algerian margin. The Boumerdès earthquake occurred on
332 a 55 km long, ENE-striking, S-dipping, reverse fault along the Algerian coast and caused a 0.7 m
333 coastal uplift. The aftershock sequence occurred on reverse but also strike-slip faults [Meghraoui *et*
334 *al.*, 2004; Ayadi *et al.*, 2008, 2010; Déverchère *et al.*, 2010]. The Tipaza earthquake occurred on an
335 ENE-striking, S-dipping, reverse, onshore fault located near the Algerian coast [Meghraoui, 1991;
336 Bounif *et al.*, 2003]. In contrast, the strongest known earthquake of the Algerian margin, i.e., the
337 1980, M 7.1 El Asnam earthquake, was generated by a NW-dipping, NE-striking reverse fault
338 located near El Asnam (Chlef), central-western Algeria [Philip and Meghraoui, 1983].

339

340 **Liguro-Provençal margin** - The Liguro-Provençal (Fig. 1) is a segmented oceanic basin
341 generated mostly during Miocene (i.e., older than the Tyrrhenian basin) in the backarc region of the
342 southeastward retreating western Mediterranean subduction zone (Fig. 2), at the rear of the counter-
343 clockwise rotating Corsica-Sardinia microplate [Gueguen *et al.*, 1998; Rollet *et al.*, 2002; Speranza
344 *et al.*, 2002; Gattacceca *et al.*, 2007; Bache *et al.*, 2010]. Extension and connected rifting in the
345 Liguro-Provençal basin started at about 25-30 Ma. Tectonics and related sedimentation study of the

346 Oligocene Provence basins provides evidence for a complex Oligocene extension history due to the
347 special situation between the western European rift and the Liguro-Provençal basin. Indeed,
348 extensional tectonics during Oligocene time up to the Chattian is related to the western European
349 rifting, whereas normal faulting that begun in the Late Chattian is influenced by the Liguro-
350 Provençal basin opening [Hippolyte *et al.*, 1993]. The 17.5-Ma-old (Ar-Ar age by Aguilar *et al.*,
351 [1996]) Beaulieu basalts (exposed about 40 km to the north of Marseille), which contain numerous
352 peridotite xenoliths, are contemporaneous with the last increments of the Oligocene to late Early
353 Miocene rifting episode that affected Provence [e.g., Hippolyte *et al.*, 1993] and that subsequently
354 led to the formation of the Ligurian-Provençal oceanic basin [e.g., Cheval *et al.*, 1989]. During the
355 Miocene, the western Alps contractional phases and structuration were still ongoing. In particular,
356 the southwestward Castellane and southward Nice compressional arcs developed during Miocene
357 and Mio-Pliocene times, respectively. In Provence, the compressional tectonics and the related
358 south-verging thrusting seemingly propagated southward from the Miocene to the Present. The
359 1909 Mw 6 earthquake represents the last reactivation of a southern Provence thrust [Trevarresse
360 fault, e.g., Lacassin *et al.*, 2002; Chardon and Bellier, 2003; Chardon *et al.* 2005].

361 Oceanic crust emplacement in the Liguro-Provençal basin occurred between about 21 and
362 16 Ma [Le Pichon *et al.*, 1971; Gueguen *et al.*, 1998; Speranza *et al.*, 2002]. Related lithosphere
363 thinning was as large as c. 50 km relative to the stable European lithosphere, which makes this
364 basin the site in the western Mediterranean with the highest acclivity of the Moho topography and
365 with an analogous topographic acclivity, i.e., from about 3000 m a.s.l. on the Argentera Massif to
366 about 2500 m u.s.l. in the oceanic floor of the Ligurian Sea [Chamot-Rooke *et al.*, 1999; Rollet *et*
367 *al.*, 2002; Tesauro *et al.*, 2008].

368 A weak but frequent seismicity has been recorded in instrumental time along the Liguro-
369 Provençal margin and in southeastern France. Historical database as well as paleoseismological
370 studies provide evidence for earthquakes with Mw 6.0-6.5 [Ferrari, 1991; Sébrier *et al.*, 1997;
371 Larroque *et al.*, 2001; Baroux *et al.*, 2003; Nguyen *et al.*, 2005; Chardon *et al.*, 2005; Cushing *et al.*,

372 2008; and SISFRANCE, e.g., Lambert *et al.*, 1996]. This seismic activity results from a N- to
373 NNW-trending compression as shown by focal mechanism solutions [Baroux *et al.*, 2001; Cushing
374 *et al.*, 2008, Larroque *et al.*, 2009], geodetic measurements [Calais *et al.*, 2002], and tectonic field
375 evidence [Hippolyte and Dumont, 2000; Champion *et al.*, 2002; Dutour *et al.*, 2002; Lacassin *et al.*,
376 2002; Chardon and Bellier, 2003; Guignard *et al.*, 2005; Chardon *et al.*, 2005].

377 Unambiguous evidence of basin inversion along the Liguro-Provençal basin margin is still
378 not available in the geological literature. One of the most suitable evidence for basin inversion is the
379 MA31 seismic reflection profile (Fig. 3c). This is a multichannel profile acquired in 1995 by
380 Ifremer (Malis Cruise) in the Ligurian basin [Bigot-Cormier *et al.*, 2004]. The profile extends from
381 the thinned continental margin of southeastern France (Nice) to the deep portion of the Liguro-
382 Provençal basin. A set of NE-dipping reflections (see the dashed red line in Fig. 3c) are interpreted
383 as a late Pliocene-Quaternary blind thrust inverting the margin of the Liguro-Provençal basin since
384 about 3.5 Ma [Bigot-Cormier *et al.*, 2004] (Table 1). This interpretation is also based on further
385 evidence including a set of offshore seismic reflection profiles showing vertical deformation and
386 southward tilting of Pliocene-Quaternary strata [Bigot-Cormier *et al.*, 2004], and fission track
387 thermochronology data suggesting a general uplift at ~3.5 Ma of the Argentera Massif [Bigot-
388 Cormier *et al.*, 2000]. Moreover, further N-dipping reverse faults are signaled onshore to the east of
389 Provence (at Capo Mele in Liguria), where these faults involve Messinian and lower Pliocene
390 sediments [Réhault, 1981; see also Sanchez *et al.*, 2010]. At the regional scale, the above-
391 mentioned Pliocene compressional deformation of the Liguro-Provençal margin is interpreted as a
392 foreland thrust propagation (i.e., the Nice arc) and Alpine front migration toward the south [Bigot-
393 Cormier *et al.*, 2004].

394 Toward the north, in the western Alpine domain, the stress regime is complicated by
395 gravitational body forces connected with the high topography and thickened crust that produce
396 forces in competition with the horizontal boundary forces, resulting in a general orogen-

397 perpendicular extension of the western Alps to the north of the Argentera Massif [Sue *et al.*, 1999;
398 Delacou *et al.*, 2008].

399

400 **South-Tyrrhenian margin** - In southern Italy, the Neogene complex convergence (and
401 associated subduction) between Eurasia and Nubia resulted in the NW-trending Apennine and W-
402 trending Maghrebian fold-thrust belts in peninsular Italy and Sicily, respectively [Malinverno and
403 Ryan, 1986; Dewey *et al.*, 1989; Patacca *et al.*, 1992]. The two belts are connected through the
404 Calabrian arc [Minelli and Faccenna, 2010], below which a narrow remnant of the former
405 subducting slab is still active, but close to cessation [Piromallo and Morelli, 2003; Mattei *et al.*,
406 2007; Neri *et al.*, 2009]. Recent marine surveys have shown that the Calabrian outer accretionary
407 wedge is still active in the Ionian offshore [Polonia *et al.*, 2008; see also Minelli and Faccenna,
408 2010]. In Sicily and southern Tyrrhenian, the Maghrebian fold-thrust belt includes two main units
409 made up of several thrust sheets mostly accreted toward the south over the Nubian foreland, locally
410 named Hyblean foreland. The two orogenic units are the innermost and structurally highest
411 Calabrian unit (mainly crystalline basement rocks) and the outermost and lowest Sicilian unit
412 (mainly basinal sequences with Tethyan ocean affinity) [Vignaroli, Rossetti *et al.*, 2008; Corrado *et*
413 *al.*, 2009; Ghisetti *et al.*, 2009]. The youngest and outermost (southernmost) thrust sheet is the
414 curved Gela Nappe, which is mostly buried beneath the foredeep infilling and the Mediterranean
415 Sea (Sicily Channel). The youngest phases of inner or basal contraction and displacements are dated
416 back to the end of early Pleistocene time [Lickorish *et al.*, 1999; Ghisetti *et al.*, 2009]. This age is
417 consistent with the hypothesized end of subduction beneath Sicily and slab breakoff (Table 1),
418 which is presumably and roughly dated with the onset of Etna's volcanism (circa 0.5 Ma), whose
419 origin is possibly connected with important discontinuities (slab windows) through the subducting
420 slab [Gvirtzman and Nur, 1999; Doglioni *et al.*, 2001; Faccenna *et al.*, 2005, 2011]. It should be
421 also noted that contraction in the Sicilian Maghrebides may still be weakly active. For instance, the

422 1968 M 6.4 Belice earthquake (central-western Sicily) has been interpreted as a compressive event
423 within the orogenic wedge [Monaco *et al.*, 1996].

424 Contraction in Sicily is, at present, mainly accommodated at the rear of the fold-thrust belt
425 in the southern Tyrrhenian (i.e., southern margin of the Tyrrhenian basin) where a series of
426 contractional earthquakes recorded during the last decades define a W-trending seismic belt [Goes
427 *et al.*, 2004; Pondrelli, Piromallo, and Serpelloni, 2004]. In particular, the epicentral and
428 hypocentral analysis of single seismic sequences pointed out that the seismically active
429 contractional structures are high-angle, N-dipping, poorly-connected, short, reverse faults (10-20
430 km in length; Billi, Presti *et al.*, 2007). The steep attitude of these faults is explained by invoking
431 the reactivation of inner thrusts that were progressively steepened by the growth, at their footwall,
432 of external thrusts during the orogenic wedge forward accretion (i.e., piggy-back sequence). Toward
433 the east, the compressional seismic belt is delimited by the seismically-active Tindari Fault, to the
434 east of which, both earthquakes and GPS data provide evidence for an ongoing extensional
435 tectonics possibly connected with the residual subduction beneath the Calabrian arc and related
436 backarc extension [Hollenstein *et al.*, 2003; D'Agostino and Selvaggi, 2004; Pondrelli, Piromallo,
437 and Serpelloni, 2004; Govers and Wortel, 2005; Billi *et al.*, 2006]. The age for the onset of the
438 ongoing contraction in the south-Tyrrhenian margin is unknown, but the cessation of volcanism at
439 Ustica (i.e., a volcanic island located along the south-Tyrrhenian contractional belt) during middle-
440 late Pleistocene time may be connected with the onset of contractional tectonics in this area. This
441 age corresponds with or is a little younger than the cessation of contractional displacements along
442 the outermost Gela Nappe in southern Sicily [Lickorish *et al.*, 1999; Ghisetti *et al.*, 2009]. It should
443 also be considered that, in the south-Tyrrhenian region, compressional events older than the one that
444 possibly started since middle-late Pleistocene time are documented [e.g. Ghisetti, 1979; Pepe *et al.*,
445 2000, 2005]. These events may be interpreted as prior rejuvenation phases of the inner orogenic
446 wedge to reestablish the taper subcriticality during the progressive continental collision in this
447 sector of the Mediterranean.

448 The high-penetration multichannel seismic reflection profile CROP M6A [Scrocca *et al.*,
449 2003; Pepe *et al.*, 2005], NNE-SSW oriented, is located across the continental margin of northern
450 Sicily (southern Tyrrhenian Sea), perpendicular to the normal listric faults that bound the Cefalù
451 basin (Fig. 4). The tectonic evolution of this margin is very complex due to the compressional-to-
452 transpressional and extensional deformation phases that took place from the early Miocene to recent
453 times. Moving from north to south, the CROP M6A profile shows the overthrusting of the KCU
454 (crystalline rocks of the Calabrian unit) on the African margin (SMU, Sicilian unit) occurred in
455 Oligocene-early Miocene time along the south-verging Drepano thrust system. In between the
456 Sicilian unit, a southeast-vergent tectonic stack occurs consisting of Meso-Cenozoic basin and
457 platform carbonate rocks and Miocene flysch of African pertinence. Following the development of
458 the northern Maghrebian belt [Pepe *et al.*, 2000, 2005 and references therein], the inner northern
459 portion of this belt, corresponding to the present-day north-Sicilian margin, was affected by the
460 onset of back-arc extensional tectonics. As an example, the Cefalù basin, recognizable at the
461 southern end of the CROP M6A profile (Fig. 4), developed on top of the accretionary complex
462 since late Tortonian-early Messinian time. Unpublished seismic reflection profiles document the
463 presence of a widespread tectonic reactivation or positive inversion of previously generated fault
464 systems since late Pliocene and throughout Quaternary times, as documented by growth strata, tilted
465 onlaps, and anomalous thickness of the Plio-Pleistocene units associated to several structural highs
466 [Scrocca *et al.*, 2006].

467

468

469 **4. EARTHQUAKES**

470 To define the main seismically-active sectors of the western Nubia-Eurasia convergent
471 margin, in Fig. 5(a) we show the map of crustal seismicity (epicenters of earthquakes with depth \leq
472 35 km and magnitude ≥ 4.0) recorded between 1962 and 2009. Earthquakes are mainly located
473 along the northern African margin (northern Morocco, Alboran Sea, and Algeria), in southern

474 Spain, in Sicily and southern Tyrrhenian Sea, and along the Apennine fold-thrust belt. Seismicity
475 becomes sparser and prevalently of small-to-moderate magnitude in Tunisia and Sicily Channel,
476 thus interrupting the continuity of the seismic belt running from the north-African margin to the
477 southern Tyrrhenian region. Sectors characterized by an almost absent seismicity are the Balearic
478 Basin and the central Tyrrhenian Sea. The Liguro-Provençal Basin is characterized by small-
479 magnitude earthquakes [Eva *et al.*, 2001; Larroque *et al.*, 2009] that are not shown in Fig. 5(a) due
480 to the magnitude threshold ($M \geq 4.0$). In the Ligurian section (east), indeed, the seismic record is
481 significantly richer in $M \geq 4.0$ earthquakes than the Provençal section (Fig. 5a). In the Italian
482 peninsula, crustal seismicity developed along a continuous belt including the Apennines, Calabrian
483 Arc, and south-Tyrrhenian margin. The seismic regime, however, changes radically from the
484 Apennines and Calabrian Arc (mainly extensional earthquakes; Chiarabba *et al.*, 2005) to the south-
485 Tyrrhenian margin (mainly compressional earthquakes to the west of the Calabrian subduction
486 zone; Pondrelli, Piromallo, and Serpelloni, 2004; Billi *et al.*, 2006, 2007) (Fig. 6).

487 Intermediate and deep seismicity (depth > 35 km) is mapped in Fig. 5(b). Subcrustal
488 earthquakes are concentrated in two main regions, which are known for active or recently active
489 subduction processes, namely the Calabrian and Gibraltar arcs [Faccenna *et al.*, 2004]. To the
490 northwest of the Calabrian Arc, in particular, intermediate and deep earthquakes are clustered and
491 aligned along a narrow (less than 200 km) and steep ($\sim 70^\circ$) Wadati-Benioff zone striking NE-SW
492 and dipping toward northwest down to 500 km of depth [Piromallo and Morelli, 2003; Neri *et al.*,
493 2009]. The subcrustal earthquakes of the Gibraltar area are interpreted as related to a relic
494 lithospheric slab dipping toward the east in the mantle beneath southern Iberia [Calvert *et al.*, 2000;
495 Gutscher *et al.*, 2002; Faccenna *et al.*, 2004].

496 Fig. 5(c) shows epicentral locations collected within the framework of the EUROSEISMOS
497 Project (http://storing.ingv.it/es_web/) for the 1900-1961 period and provides a general overview of
498 the seismicity during the last century before the advent of modern seismic networks. Fig. 5(c)
499 confirms the seismic activity, rather energetic in some instances, of southern Iberia, Algeria, and

500 Italy. No earthquakes are reported for northern Morocco, Tunisia, and southern Tyrrhenian, but this
501 evidence is possibly due to the poor coverage of seismic networks [Buforn *et al.*, 1988; Giardini *et*
502 *al.*, 2002]. In contrast to what observed in Fig. 5(a), during 1900-1961, $M \geq 4$ earthquakes were
503 recorded also in the Liguro-Provençal area, southern France (Fig. 5c).

504 Fig. 6 shows the focal mechanisms of the earthquakes with magnitude ≥ 4.5 available for the
505 study region since 1976. The chosen magnitude threshold allows us to obtain insights into regional
506 scale geodynamic processes rather than local ones. Data of Fig. 6(a) are taken from the Harvard
507 Centroid-Moment Tensors (CMT) catalog (<http://www.globalcmt.org/CMTsearch.html>) and
508 provide robust, stable, and reliable seismic source mechanisms based on the fitting of long period
509 seismic waveforms recorded at the global scale [Dziewonski *et al.*, 1981, 2000]. The CMT data
510 have been integrated with data from the European-Mediterranean Regional Centroid Moment
511 Tensor (RCMT) catalog (<http://www.bo.ingv.it/RCMT/>) for the 1997-2004 period (Fig. 6b). The
512 RCMT catalog is based on the fitting of surface waves with intermediate and long period recorded
513 at regional distance and its quality evaluation processes ensure high-reliability of data [Pondrelli *et*
514 *al.*, 2002, 2004, 2006, 2007]. The CMT catalog provides moment tensors for earthquakes with $M >$
515 5, whereas the RCMT procedure involves data from earthquakes with magnitude as small as 4.2.
516 Different colors for focal mechanisms (Fig. 6) indicate different types of mechanisms according to
517 the Zoback's classification adopted for the World Stress Map (<http://dc-app3-14.gfz-potsdam.de/>;
518 Zoback, 1992). Figs. 6(a) and 6(b) show that reverse faulting is the main style of seismic
519 deformation along the Nubia-Eurasia margin between Gibraltar and Sicily. The focal mechanisms
520 available for the southern Tyrrhenian area indicate reverse displacements as the main or solely
521 seismic mechanism active in this area, whereas, moving toward the Algerian margin, earthquakes
522 with thrust mechanisms are associated to several transpressional and strike-slip earthquakes, which
523 become dominant in the Betics, northern Morocco, and Alboran Sea [Lammali *et al.*, 1997;
524 Bezzeghoud and Buforn, 1999; Henares *et al.*, 2003; Vannucci *et al.*, 2004; Billi, Presti *et al.*,
525 2007]. The above-depicted focal features are synthesized in the polar plots of P- and T-axes selected

526 by source areas (Fig. 6c). Seismic activity in the south Tyrrhenian belt occurred in response to a
527 NNW-SSE oriented compressive stress, which is also predominant in northern Algeria together
528 with some evidence of WSW-ENE extension. Toward the west (Betics, northern Morocco, and
529 Alboran Sea), in contrast, a WSW-ENE extension becomes predominant. Evidence of seismic
530 reverse faulting is also present in Tunisia (E-W compression), off eastern Sardinia (E-W
531 compression), and southeastern France (N-S compression). To the east of the study area, focal
532 mechanisms and plots of P- and T-axes (Fig. 6) from the Apennines and Adriatic Sea show the post-
533 orogenic extension active in the Apennines in response to a regional NE-SW extension [Montone *et*
534 *al.*, 2004; Pondrelli *et al.*, 2006], and the compressional seismic displacements active mainly in the
535 eastern side of the Adriatic block (in response to a NNE-SSW regional compression) but also in the
536 mid-Adriatic area and Gargano promontory, where compressional-to-transpressional earthquakes
537 are also recorded [Montone *et al.*, 2004; Billi *et al.*, 2007].

538

539

540 **5. KINEMATICS FROM GPS DATA**

541 The precise measurement of plates and microplates kinematics through the use of modern
542 GPS networks has significantly influenced most recently proposed interpretations concerning the
543 tectonics and geodynamics of the Nubia-Eurasia plate boundary in the Mediterranean area.
544 Although the number of GPS sites in the western Mediterranean region has remained quite limited
545 until a few years ago, the number of available GPS networks has significantly increased in the last
546 five years in most European countries, particularly in Italy, thanks to the development of new
547 networks devoted to both geophysical and topographical issues. Unfortunately, the same progress is
548 not true for the northern African countries, where the number of GPS data and measurements is still
549 sparse or absent.

550 Although the number of GPS networks specifically designed for geophysical purposes is
551 still limited compared with the number of networks developed for topographic goals, the optimal

552 combination of all available data has recently provided an increasing number of details concerning
553 the kinematics of plates and microplates in the central and western Mediterranean [Hollenstein *et*
554 *al.*, 2003; D'Agostino and Selvaggi, 2004; Serpelloni *et al.*, 2005; Stich *et al.*, 2006; Serpelloni *et*
555 *al.*, 2007; D'Agostino *et al.*, 2008].

556 Here we present a horizontal velocity field at the scale of the western Mediterranean
557 obtained from the combination of published and original GPS velocities (Fig. 7). We used the
558 GAMIT/GLOBK [Herring *et al.*, 2006] software to process data from continuously operating GPS
559 (CGPS) networks in Italy and surrounding regions, following standard procedures for regional
560 networks [Serpelloni *et al.*, 2006, 2007]. By analyzing position time series originally defined in the
561 IGS realization of the ITRF05 reference frame [Altamimi *et al.*, 2007], we estimated velocities
562 together with seasonal (i.e., annual and semiannual) signals and offsets due to instrumental changes.
563 We used high quality CGPS sites in central Europe (characterized by longer time-series and low
564 position scatters) to define a fixed Eurasian reference frame (located at Longitude $-98.85 \pm 0.24^\circ\text{E}$,
565 Latitude $54.74 \pm 0.30^\circ\text{N}$ and with rotation rate of $0.257 \pm 0.001^\circ/\text{My}$).

566 In Fig. 7(a), we present only horizontal velocities obtained from the time-series modeling of
567 high quality CGPS networks (i.e., originally developed for geophysical or geodetic studies), of
568 which the backbone network is represented by the INGV-RING stations [Avallone *et al.*, 2010],
569 integrated by other regional geodetic networks, including the ASI, EUREF and FredNet (see
570 Serpelloni *et al.*, [2006]; and Avallone *et al.*, [2010] for more details). Velocity uncertainties were
571 estimated adopting a white+flicker noise model [Williams *et al.*, 2004]. We used, however, only
572 CGPS stations presenting more than three years of measurements. It is worth noting that the
573 distribution of CGPS sites in the western Mediterranean basin is largely heterogeneous, making the
574 analysis of crustal strain-rates at the plate boundary scale quite challenging. To improve the spatial
575 resolution of our velocity field, for northern Africa and southern Iberia, we used also previously-
576 published GPS velocities [Stich *et al.*, 2006; Serpelloni *et al.*, 2007; Tahayt *et al.*, 2008; Peña *et*
577 *al.*, 2010], which are rigorously aligned to our Eurasia-fixed reference frame. To compute the 6-

578 parameters (3 rotations and 3 translations) Helmert transformation and align the published velocity
579 fields to our Eurasian-fixed frame realization, we used GPS sites that are common to our solution
580 and to the published ones (mostly belonging to the EUREF of IGS networks).

581 Fig. 7(a) shows the horizontal velocities given with respect to Eurasia, together with plate
582 motion vectors predicted by the estimated Nubia-Eurasia relative rotation pole, at points in northern
583 Africa for which one can assume a purely rigid behavior. Clearly, the number of available GPS
584 velocity vectors in Italy is significantly larger than the remaining area, so only long wavelength
585 features of the crustal strain rate field can be reasonably investigated at the western-Mediterranean
586 scale.

587 We used the approach described in Shen *et al.* [1996], which accounts for velocity
588 uncertainties, network geometry, and inter-station distances, to estimate the velocity gradient field.
589 Horizontal strain-rate tensors at points of a regular grid ($0.25^\circ \times 0.25^\circ$ spacing), extending between
590 longitude $8.0E^\circ$ - $14.5E^\circ$ and latitude $42.0N^\circ$ - $46.0N^\circ$, are estimated from the velocity data through
591 weighted least squares. Velocities are re-weighted by a Gaussian function $\exp(-\Delta R^2/D^2)$, where
592 ΔR is the distance between a geodetic station and the grid point being evaluated and D is a
593 smoothing distance that is optimally determined in this algorithm (between a priori defined lower
594 and upper bound) through balancing the trade-off between the formal strain rate uncertainty
595 estimate and the total weight assigned to the data [Shen *et al.*, 2007]. In this way, measurements
596 made closer to a grid point contribute more to the strain estimate at that point, and the smoothing is
597 applied according to the station distribution and density. The re-weighting determines the degree of
598 smoothing around a given spot and the uncertainties of the strain estimates, while the optimally
599 determined D value can be considered as an indicator of how “locally” or “regionally” determined
600 is the strain-rate tensor inverted at each grid point. Given the largely heterogeneous distribution of
601 GPS stations in the investigated area, we aim at illuminating the long-wavelength features of the
602 velocity gradient field using a starting D value of 80 km (i.e., features of wave-length lower than 80

603 km are filtered out by spatial smoothing), obtaining values ranging between 80 and 400 km, and an
604 average value of 142 km.

605 Fig. 7(a) shows the horizontal velocities (with 95% uncertainties) obtained from the
606 combination of original data (in the central Mediterranean) and published velocities (in the western
607 Mediterranean), together with the velocities interpolated over the regular grid, as obtained from our
608 least-squares estimates of the velocity gradient field. Fig. 7(b) shows the horizontal strain-rate field,
609 i.e., the maximum and minimum eigenvectors of the strain-rate tensors.

610 The most evident kinematic features is the motion toward the northwest of the Nubian plate,
611 with respect to Eurasia, and the progressive clockwise rotation of the velocity vectors toward the
612 central Mediterranean, i.e., from northwestward in the western Mediterranean (Morocco) to
613 northeastward in the central Mediterranean (Calabria). Further “local” deviations from this
614 kinematic pattern are observed in northern Morocco and Alboran basin, and also in northeastern
615 Sicily and northern Calabria, where fast deformation rates occur. In particular, if SW-NE oriented
616 shortening is observed along the Moroccan Rif, extension, mainly E-W oriented, characterizes the
617 western Alboran basin and southern Iberia. In northern Algeria and Tunisia, the lack of a good
618 coverage of GPS sites prevents any detailed estimate of the contemporary strain-rate field.
619 However, a few sites along the coast of northern Algeria suggest that this segment of the Nubia-
620 Eurasia plate boundary accommodates about 2-4 mm/yr of SE-NW convergence [Serpelloni *et al.*,
621 2007]. Moving toward the east, while N-S shortening characterizes the Sardinia Channel, a few
622 available sites make this features purely interpolated and representative of broad geodynamic
623 features. Fast N-S shortening characterizes the southern Tyrrhenian basin, where the fastest
624 deformation rates are observed in the central Aeolian area (southeastern Tyrrhenian Sea). In Sicily,
625 the northward velocities suggest a SW-NE extension between mainland Sicily and the Nubian plate.
626 This extension, which is of the order of 1.5÷2 mm/yr, is likely accommodated across the Pantelleria
627 Rift system in the Sicily Channel. Large extensional deformation rates are observed in northeastern
628 Sicily and southern Calabria, where a sudden change in the velocity trends, which change from

629 northward to northeastward, are accommodated mainly across the Messina straits and also across
630 the Cefalù-Etna seismic belt in Sicily [Pondrelli, Piromallo, and Serpelloni, 2004; Billi *et al.*, 2010].

631 Along the Italian peninsula, the velocity field is mainly characterized by two distinct trends.
632 Sites located on the Tyrrhenian side of the Apennine chain move toward the northwest, whereas
633 sites located on the Adriatic side of the chain move toward the north-northeast. This differential
634 motion results in the SW-NE oriented extensional deformation that characterizes the Apennines
635 chain [Montone *et al.*, 2004].

636 Across the Liguro-Provençal basin, GPS data show no significant deformation rates. In
637 particular, no active extension is observed between the Corsica-Sardinia block and the coasts of
638 southern France and Spain. Only a very limited, but statistically not significant, NW-SE shortening
639 is observed north of Barcelona.

640

641

642 **6. DISCUSSION**

643 We cannot predict the future evolution and final setting of what will be the Nubia-Eurasia
644 suture in the western Mediterranean with the progression of plate convergence. A glance at the
645 present setting of this area (Fig. 1), in fact, points out the strong heterogeneity and non-cylindricity
646 of physiography and tectonic structures along this boundary, whose evolution will be therefore
647 highly non-cylindrical as it has been so far since at least Paleogene time [Faccenna *et al.*, 2004]. We
648 can provide, however, some significant insights into the recent evolution of this boundary to attempt
649 understanding what will be its progression in the near future.

650 The spatio-temporal evolution of the studied segment of the Nubia-Eurasia boundary
651 indicates that its past evolution has been obviously influenced by the Nubian subduction (Fig. 2).
652 To understand a possible future progression of this boundary it is therefore necessary to know the
653 present state of the Nubian subduction beneath Eurasia. To do so, we reconsidered a previously
654 published tomographic model of the western Mediterranean [Piromallo and Morelli, 2003].

655 Fig. 8 shows five horizontal layers (150-to-500 km deep) extracted from the tomographic
656 model PM0.5, whose thorough description is provided by Piromallo and Morelli [2003] and
657 Faccenna *et al.*, [2004]. The model, which encompasses the upper mantle beneath the western
658 Mediterranean region, is obtained by inversion of regional and teleseismic P wave residuals from
659 the International Seismological Centre Bulletin. In the upper layers, we observe a high seismic
660 velocity (i.e., positive) anomaly running discontinuously from the northern Apennine, turning
661 around the Calabrian Arc, and heading toward the Gibraltar Arc. We interpret this high velocity
662 volume as the cold lithosphere sunk (subducted) in the mantle along the convergent boundary
663 between Nubia and Eurasia in the western Mediterranean [Wortel and Spakman, 2000; Faccenna *et*
664 *al.*, 2004]. At 150 km depth (Fig. 8), the high-velocity anomaly is located beneath the northern-
665 central Apennines, Calabria, northern Algeria, and the Gibraltar Arc. Evident lateral interruptions of
666 this structure occur in three regions, namely beneath the southern Apennines, the Sicily Channel
667 and the Oranie-Melilla region, where low velocity anomalies occur [Faccenna *et al.*, 2004]. The
668 first two gaps (Apennines and Sicily Channel) close at larger depths. At 250 km depth, the Calabria
669 high-velocity anomaly merges, toward the north-east, with the Apennines and, toward the west,
670 with the Algerian anomalies (see the 250 km layer in Fig. 8). The westernmost interruption (Oranie-
671 Melilla), conversely, persists down to about 400-450 km depth (see deep layers in Fig. 8). The high-
672 velocity anomaly belt detected by tomography (Fig. 8) is therefore laterally fragmented beneath the
673 southern flank of the Gibraltar and Calabrian arcs, where deep slab breaks line up with the main
674 discontinuities in the geological trends, i.e., the Sicily Channel and the Oranie-Melilla region. At
675 about 500 km depth (Fig. 8), the high-velocity anomaly spreads horizontally over the whole western
676 Mediterranean area, whereas no coherent trace of high-velocity anomaly is present below 670 km
677 depth. This evidence suggests that the material pertaining to different subduction zones is ponding
678 at the upper/lower mantle discontinuity [Wortel and Spakman, 2000; Piromallo *et al.*, 2001;
679 Piromallo and Faccenna, 2004].

680 The tomographic model (Figs. 8 and 9) shows that the Nubian subduction beneath Eurasia in
681 the western Mediterranean is, after millions of years of efficiency and accommodation of plate
682 convergence, now largely discontinuous. Several studies agree that subduction is here progressively
683 decaying, thus becoming poorly- or non-operative [e.g., Wortel and Spakman, 2000; Faccenna *et*
684 *al.*, 2004; Neri *et al.*, 2009]. As plate convergence is nonetheless still operative at rates between
685 about 1 and 5 mm/y [Nocquet and Calais, 2004; Serpelloni *et al.*, 2007], a new tectonic
686 reorganization is presently in progress in the western Mediterranean to accommodate such a
687 convergence. The original and previously-published evidence presented in this paper help us
688 understanding such a tectonic reorganization.

689 Although rather diffuse, the contractional deformation in the western Mediterranean (as
690 inferred from seismicity, Figs. 5 and 6) tends to concentrate at the margins of the oceanic backarc
691 basins (i.e., Algeria and southern Spain, Liguria-Provence, and southern Tyrrhenian), where the
692 rheological contrast between adjacent continental and oceanic domains as well as other factors such
693 as the geometric and thermomechanical properties of the transitional crust controls and favors the
694 localization of contractional deformation [e.g., Béthoux *et al.*, 2008]. The Alboran basin, in
695 contrast, where no oceanic crust occurs (at least in the western section), has undergone a diffuse
696 inversion tectonics since about 8 Ma. Hypothesizing a future subduction of this basin seems,
697 therefore, irrational. Concerning the two oceanic backarc basins, whether the final suture between
698 Nubia and Eurasia will be reached through their closure and subduction is highly debatable, among
699 other reasons, because of the young age (i.e., temperature and density poorly appropriate for
700 subduction) and reduced dimensions of these basins [Erickson and Arkani-Hamed, 1993; Cloos,
701 1993]. A thermomechanical modeling of these basins to infer their potential aptitude to being
702 subducted is beyond our scopes. As, however, some evidence suggests subduction inception across
703 segments of the basin margins (e.g., off Algeria; Strzeczynski *et al.*, [2010]), we assume subduction
704 will be the process toward which plate tectonics is heading to in the western Mediterranean,
705 regardless of whether a complete subduction of the Algerian-Liguro-Provençal and Tyrrhenian

706 oceanic basins will ever be accomplished. Upon this assumption, the geological and geophysical
707 evidence presented in this paper provides insights into the subduction inception, which is, in
708 general, a process still poorly known for the substantial absence of instructive instances on the Earth
709 [Cloething *et al.*, 1982, 1990; Shemenda, 1992; Toth and Gurnis, 1998; Faccenna *et al.*, 1999;
710 House *et al.*, 2002].

711 Backarc basin inversion in the western Mediterranean started at about 8 Ma from the west
712 (Alboran and Algerian margins) following a substantial cessation of subduction (Table 1), and then
713 propagated toward the east up to the present time, also in this case as the consequence of a
714 substantial cessation of subduction beneath Sicily (Faccenna *et al.*, 2004; Fig. 9). This spatio-
715 temporal migration (from west to east since about 8 Ma) allows us to provide insights into the
716 process of subduction inception at different temporal stages (i.e., disregarding tectonic differences
717 between inverted margins). Starting from the youngest margin (Tyrrhenian), where pre-existing and
718 presumably-weak reverse faults occur, these faults are possibly reactivated before inversion and
719 then subduction of the Tyrrhenian margin will start. The seismic activity in the south-Tyrrhenian
720 margin occurs, in fact, along inner S-verging reverse faults (i.e., vergence opposite to that expected
721 for the hypothesized subduction of the Tyrrhenian basin) of the Maghrebian belt, which is therefore
722 being rejuvenated at its rear [Billi, Presti *et al.*, 2007]. Also in the Algerian margin, where basin
723 inversion (*sensu stricto*) and possibly subduction inception have already started with newly
724 generated reverse faults verging toward the north, reverse faults verging toward the south and
725 possibly inherited from the Paleogene-Neogene contractional phases are still active with associated
726 seismic release [e.g., Mauffret, 2007]. It follows that subduction inception (i.e., the formation of a
727 new plate boundary) is possibly an energetically-consuming process [Toth and Gurnis, 1998],
728 which is substantially anticipated by less consuming processes such as the reactivation of inner
729 thrusts up to the ultimate locking of the orogenic wedge and subsequent transfer of contraction to
730 the backarc basin margin heading for a subduction inception. A viable model of subduction
731 inception (supported by the diachronous age of backarc compression onset) may be the lateral

732 propagation, in a scissor-like fashion, of the new plate boundary where subduction is progressively
733 initiated (Fig. 10). Moreover, our GPS data show that strain rates across the studied boundary are
734 laterally very heterogeneous. In particular, contractional strain rates computed for the south-
735 Tyrrhenian region are significantly larger than those for the Algerian margin. This evidence is
736 difficult to interpret. One explanation may simply be connected with the poor coverage of GPS
737 stations in northern Africa. An alternative explanation may be that contraction accommodation
738 through reactivation of pre-existing reverse faults (south-Tyrrhenian; Pepe *et al.*, [2005]; Billi,
739 Presti *et al.*, [2007]) is more efficient than subduction inception and basin inversion along newly-
740 generated reverse faults (Algeria; Strzeczynski *et al.*, [2010]). The heterogeneous strain rates and
741 GPS velocities implies that, probably, the Sicilian domain is moving independently by the Nubian
742 domain (Algeria) and that a transcurrent (right-lateral)-to-extensional decoupling zone in the Sicily
743 Channel area should enable such differential movements [Serpelloni *et al.*, 2007].

744 Assuming that, from west to east, since about 8 Ma, the Nubia-Eurasia convergence has
745 been mainly accommodated through backarc basin inversion (and perhaps subduction inception off
746 Algeria), we expect the following horizontal displacements (i.e., heaves normal to the new plate
747 boundary), which are calculated from the displacement trajectories of Africa with respect to stable
748 Eurasia [Dewey *et al.*, 1989; Faccenna *et al.*, 2004]: c. 25 km across the Alboran basin since about
749 8 Ma and c. 15 km across the Algerian basin since about 5 Ma. As above pointed out, the
750 contractional displacement in the Alboran basin is non-localized, whereas the one off Algeria is
751 rather localized and may have partly contributed to subduction inception. From the above-estimated
752 displacements, we obtain displacement rates of about 3.1-3.2 mm/y, which are consistent with the
753 present GPS velocities of Nubia (Fig. 7). For the south-Tyrrhenian margin, the expected horizontal
754 contractional displacement since 0.5 Ma has already been assessed as about 2.5 km [Billi, Presti *et*
755 *al.*, 2007] by assuming the present GPS velocity of Nubia with respect to fixed Eurasia (c. 5 mm/y
756 for the south-Tyrrhenian-Sicilian region) as constant during the last 500 ky and the motion of Nubia
757 during this period as entirely accommodated across the south-Tyrrhenian deformation zone.

758 The Liguro-Provençal northern margin is different from the Algerian and Tyrrhenian
759 margins for several reasons. The Liguro-Provençal is, geodynamically, an oceanic backarc basin
760 developed at the rear of the south- and southeast-verging Apennine-Maghrebian belt and
761 anticlockwise rotating Corsica-Sardinia block, but, at the same time, it can be considered as the
762 foreland of the south-verging southwestern Alpine front (i.e., the Nice arc). Therefore, unlike the
763 active tectonics of the south-Tyrrhenian margin, the ongoing compression along the Liguro-
764 Provençal margin can be considered as a resumption of the Alpine thrust propagation toward the
765 foreland and not a rejuvenation at the rear of the belt (either Alpine or Apennine) as it happens in
766 the Tyrrhenian and, partly, in the Algerian margins. The reason why the Liguro-Provençal basin is
767 presently undergoing compression (as evidenced by a seismicity significantly larger than that in the
768 surrounding areas) is still matter of debate [Béthoux *et al.*, 1992; Sue *et al.*, 1999; Larroque *et al.*,
769 2009], but the hypothesis of a thermomechanical weakness of this region is a viable one [Béthoux *et*
770 *al.*, 2008]. Assuming this hypothesis as true, part of the contractional deformation would have been
771 transferred from the Sicily Channel (i.e., the area between northern Tunisia and northern Sicily
772 where seismicity is weaker than that in the adjacent segments of the Nubia-Eurasia boundary),
773 where no thinned oceanic crust occurs, to the north in the weaker oceanic domain of the Liguro-
774 Provençal basin [Billi, Presti *et al.*, 2007; Serpelloni *et al.*, 2007; Larroque *et al.*, 2009; Billi *et al.*,
775 2010]. Due to the largely inhomogeneous distribution of GPS stations along the studied boundary
776 and hence to the choice of analyzing only the most significant longer wavelengths strain-rate
777 features, our GPS data for the Liguro-Provençal margin show no significant deformation rates (Fig.
778 7). A local geodetic study, however, pointed out a weak (c. 1 mm/y) contraction in the Provençal
779 region [Calais *et al.*, 2002; Nocquet and Calais, 2004] consistently with the recorded compressional
780 earthquakes [Baroux *et al.*, 2001; Larroque *et al.*, 2009] and with a recent seismological analysis
781 indicating a strain rate of c. $3 \times 10^{-9} \text{ y}^{-1}$ for the Ligurian Sea (i.e., note that not all deformation is
782 seismic; Barani *et al.* 2010). It should also be considered that the onset of basin inversion (c. 3.5
783 Ma) in the Liguro-Provençal margin is younger than the same type of tectonics in the Algerian

784 margin (c. 6-7 Ma), but older than the compression resumption in the south-Tyrrhenian margin
785 (younger than c. 2 Ma). This evidence suggests that basin inversion in the Liguro-Provençal margin
786 is in the wake of the spatio-temporal tectonic reorganization of the western Mediterranean after the
787 substantial cessation of Nubian subduction and, therefore, is part of this new reorganization heading
788 for the inversion and closure of the western Mediterranean.

789 Alternative, viable interpretations for the contractional tectonics in the northern Liguro-
790 Provençal margin involve isostasy/buoyancy forces rather than Nubia-Eurasia plate tectonic
791 collision, and anticlockwise rotation of the Apulian plate [Sue *et al.*, 1999; Sue and Tricart, 2003;
792 D'Agostino *et al.*, 2008; Delacou *et al.*, 2008]. We propend for our model (i.e., accommodation of
793 Nubia-Eurasia convergence also in the Liguro-Provençal basin) on the basis of the spatio-temporal
794 evolution of the compressional wave from west to east (i.e., basin inversion; Fig. 9) and on the basis
795 of substantial absence of compressional tectonics between Tunisia and northwestern Sicily
796 (northwestern Sicily Channel), this latter evidence suggesting that the compression has to be
797 somehow redistributed, for instance shifting it toward the north in the Liguro-Provençal basin. We
798 acknowledge, however, that the debate on the cause of the Liguro-Provençal compressional
799 tectonics is still open and the evidence still weak to unambiguously support a single model.

800 It should eventually be noted that part of the contractional displacements are transferred to
801 the north not only in the Liguro-Provençal region, but also in the Alboran-Algerian basin. The
802 portion of southern Spain facing the Alboran-Algerian basin between about Alicante and Malaga, in
803 fact, is presently undergoing compression [Fernández-Ibáñez *et al.*, 2007; Serpelloni *et al.*, 2007].

804 The above-discussed tectonic reorganization of the western Mediterranean together with
805 some local tectonic evidence [e.g., Pepe *et al.*, 2005; Billi, Presti *et al.*, 2007; Strzeczynski *et al.*,
806 2010] points out the segmentation of the new incipient boundary, where inherited structures and
807 lateral crustal heterogeneities prevent, at the present stage, the development of a continuous long
808 convergent boundary consisting of thrust faults and an incipient subduction zone. If compression,
809 basin inversion, and subsequent inception of subduction will continue in the presently active

810 margins (i.e., east Alboran, Algerian, Liguro-Provençal, and south-Tyrrhenian; Fig. 9), we may
811 hypothesize, in about 1500 km of convergent boundary (from east-Alboran to Tyrrhenian), a slab
812 dip reversal (southward in the Algerian and south-Tyrrhenian margins and northward in the Liguro-
813 Provençal margin) and a subduction zone spatial shift of about 600 km (the N-S distance between
814 the Algerian and Liguro-Provençal margins).

815 In synthesis, the above-discussed past evolution and hypothesized future scenario for the
816 western Mediterranean outlines a process similar to the Wilson Cycle (at a small scale), i.e., the
817 opening and closing of ocean basins [Wilson, 1963]: (1) northward Nubian subduction with
818 Mediterranean backarc extension (since ~35 Ma); (2) progressive cessation, from west to east, of
819 Nubian main subduction (since ~15 Ma); (3) progressive onset of compression, from west to east, in
820 the former backarc domain and consequent basin inversion (since ~8-10 Ma); (4) possible future
821 subduction of former backarc basins.

822

823

824 **7. CONCLUSIONS**

825 Basin inversion, subduction, and thrusting on ocean-scale convergent boundaries, which
826 may be at the origin of strong earthquakes and related tsunamis, are tectonic processes rather well
827 known from several geologic and geophysical data. The nucleation modes and infant stages of these
828 processes and related structures, however, are far less known for the paucity of evidence and
829 uncertainty on where, on the Earth, these processes and structures are going to nucleate soon.

830 The geologic and geophysical evidence presented in this paper indicate that the western
831 Mediterranean is a suitable region to study the onset of basin inversion that may possibly lead to
832 subduction inception and to the final suture between Nubia and Eurasia in the study region. The
833 same evidence reveal also some insights into the recent and present processes such as the lateral
834 (scissor-like) migration of backarc inversion from west to east following a similar migration of
835 subduction cessation, and the transfer of inversion tectonics toward the north in a weaker strand

836 (i.e., Provence and Liguria) of the basin margin (Table 1). These insights will be useful to
837 understand future tectonic scenarios in the western Mediterranean. An improvement of the geodetic
838 and seismic networks (e.g., marine stations, see Dessa *et al.*, [2011]) is, however, mandatory to
839 better understand the kinematics and deformation rates of the studied boundary, thus possibly
840 contributing to the knowledge of earthquake and tsunami hazard and to the assessment of their
841 effects.

842

843

844 **Acknowledgments:** L. Jolivet and an anonymous reviewer are warmly thanked for constructive
845 reviews. Scientific exchanges and discussions with S. Cloetingh, J. Déverchère, R. Govers, R.
846 Wortel, and many other colleagues were very useful. B. Guillaume helped with Fig. 9. This work
847 was realized within the framework of the TopoMed Project led by R. Wortel. TopoMed is part of
848 the ESF EUROCORES Topo-Europe Programme (www.topo-europe.eu) led by S. Cloetingh.

849 **References**

- 850 AGUILAR J.-P., CLAUZON G., DE GOËR DE HERVÉ A., MALUSKI H.J., M. & WELCOMME J.-L. (1996). - The MN3 fossil
851 mammal-bearing locality of Beaulieu (France): Biochronology, radiometric dating, and lower age limit of the
852 early Neogene renewal of the mammalian fauna in Europe. - *Newsl. Stratigr.*, **34**, 177-191.
- 853 ALLEN M., JACKSON J. & WALKER R. (2004). - Late Cenozoic reorganization of the Arabia-Eurasia collision and the
854 comparison of short-term and long-term deformation rates. - *Tectonics*, **23**, TC2008,
855 doi:10.1029/2003TC001530.
- 856 ALTAMIMI Z., COLLILIEUX X., LEGRAND J., GARAYT B. & BOUCHER C. (2007) - ITRF2005: A new release of the
857 International Terrestrial Reference Frame based on time series of station positions and Earth Orientation
858 Parameters. - *J. Geophys. Res.*, **112**, B09401, doi:10.1029/2007JB004949.
- 859 AUZENDE J.-M., BONNIN J. & OLIVET J.L. (1975). - La marge nord-africaine considérée comme marge active. - *Bull.*
860 *Soc. géol. Fr.*, **17**, 486-495.
- 861 AVALLONE A., SELVAGGI G., D'ANASTASIO E., D'AGOSTINO N., PIETRANTONIO G., RIGUZZI F., SERPELLONI E.,
862 ANZIDEI M., CASULA G., CECERE G., D'AMBROSIO C., DE MARTINO P., DEVOTI R., FALCO L., MATTIA M., ROSSI
863 M., OBRIZZO F., TAMMARO U. & ZARRILLI L. (2010). - The RING network: improvements to a GPS velocity
864 field in the central Mediterranean. - *Ann. Geophys.*, **53**, doi: 10.4401/ag-4549.
- 865 AYADI A., DORBATH C., OUSADOU F., MAOUCHE S., CHIKH M., BOUNIF M.A. & MEGHRAOUI M. (2008). - Zemmouri
866 earthquake rupture zone (Mw 6.8, Algeria): Aftershocks sequence relocation and 3D velocity model. - *J.*
867 *Geophys. Res.*, **113**, B09301, doi:10.1029/2007JB005257.
- 868 AYADI A., DORBATH C., OUSADOU F., MAOUCHE S., CHIKH M., BOUNIF M.A. & MEGHRAOUI M. (2010). - Reply to
869 comment by J. Déverchère et al. On "Zemmouri earthquake rupture zone (Mw 6.8, Algeria): Aftershocks
870 sequence relocation and 3D velocity model". - *J. Geophys. Res.*, **115**, B04319, doi:10.1029/2009JB006705.
- 871 BACHE F., OLIVET J.L., GORINI C., ASLANIAN D., LABAILS C. & RABINEAU M. (2010). - Evolution of rifted continental
872 margins: the case of the Gulf of Lions (western Mediterranean basin). - *Earth Planet Sc. Lett.*, **292**, 345-356.
- 873 BARANI S., SCAFIDI D. & EVA C. (2010). - Strani rates in northwestern Italy from spatially smoothed seismicity. *J.*
874 *Geophys. Res.*, doi:10.1029/2009JB006637.
- 875 BAROUX E., BÉTHOUX N. & BELLIER O. (2001). - Analyses of the stress field in southeastern France from earthquake
876 focal mechanisms. - *Geophys. J. Int.*, **145**, 336-348.
- 877 BAROUX E., PINO N.A., VALENSISE G., SCOTTI O. & CUSHING M. (2002). - Source parameters of the 11 June 1909,
878 Lambesc (Souther France) earthquake: a reappraisal based on macroseismic, seismological and geodetic
879 observations. - *J. Geophys. Res.*, **108**, 2454, doi:10.1029/2002JB002348.
- 880 BÉTHOUX N., FRÉCHET J., GUYOTON F., THOUVENOT F., CATTANEO M., EVA C., NICOLAS M. & GRANET M. (1992). A
881 closing Ligurian Sea? - *Pure Appl. Geophys.*, **139**, 179-194.
- 882 BENOUAR D. (2004). - Materials for the investigation of historical seismicity in Algeria from the records of past
883 earthquakes. *Ann. Geophys.*, **47**, 555-560.
- 884 BÉTHOUX N., TRIC E., CHERY J. & BESLIER M.-O. (2008). - Why is the Ligurian basin (Mediterranean Sea)
885 seismogenic? Thermomechanical modeling of a reactivated passive margin. - *Tectonics*, **27**, TC5011,
886 doi:10.1029/2007TC002232.
- 887 BEZZEGHOUD M., AYADI A., SEBAI A., AIT MESSAOUD M., MOKRANE A. & BENHALLOU H. (1996) - Seismicity of
888 Algeria between 1365 and 1989: Map of Maximum Observed Intensities (MOI). *Avances en Geofisica y*
889 *Geodesia*, **I**, IGN, Madrid, 107-114.
- 890 BEZZEGHOUD M. & BUFORN E. (1999). - Source parameters of the 1992 Melilla (Spain, Mw 4.8), 1994 Alhoceima
891 (Morocco, Mw 5.8) and 1994 Mascara (Algeria, Mw 5.7) earthquakes and seismotectonic implications. *Bull.*
892 *Seism. Soc. Am.*, **89**, 359-372.
- 893 BIGOT-CORMIER F., POUPEAU G. & SOSSON M. (2000). - Dénudations différentielles du massif externe alpin de
894 l'Argentera (Sud-Est de la France) révélée par thermochronologie traces de fission (apatites, zircons). - *C. R.*
895 *Acad. Sci. Paris*, **330**, 363-370.
- 896 BIGOT-CORMIER F., SAGE F., SOSSON M., DEVERCHERE J., FERRANDINI M., GUENNOG P., POPOFF M. & STEPHAN J.F.
897 (2004). - Déformations pliocènes de la marge nord-Ligure (France): Les conséquences d'un chevauchement
898 crustal sud-alpin. - *Bull Soc. géol. Fr.*, **175**, 197-211.
- 899 BILLI A., BARBERI G., FACCENNA C., NERI G., PEPE F. & SULLI A. (2006). - Tectonics and seismicity of the Tindari
900 Fault System, southern Italy: Crustal deformations at the transition between ongoing contractional and
901 extensional domains located above the edge of a subducting slab. - *Tectonics*, **25**, TC2006,
902 doi:10.1029/2004TC001763.
- 903 BILLI A., GAMBINI R., NICOLAI C. & STORTI F. (2007). - Neogene-Quaternary intraforeland transpression along a
904 Mesozoic platform-basin margin: the Gargano fault system, Adria, Italy. - *Geosphere*, **3**, 1-15.
- 905 BILLI A., PRESTI D., FACCENNA C., NERI G. & ORECCHIO B. (2007). - Seismotectonics of the Nubia plate compressive
906 margin in the south-Tyrrhenian region, Italy: clues for subduction inception. - *J. Geophys. Res.*, **112**, B08302,
907 doi:10.1029/2006JB004837.

- 908 BILLI A., PRESTI D., ORECCHIO B., FACCENNA C. & NERI G. (2010). - Incipient extension along the active convergent
909 margin of Nubia in Sicily, Italy: the Cefalu-Etna seismic zone. - *Tectonics*, **29**, TC4026,
910 doi:10.1029/2009TC002559.
- 911 BOUNIF A., BEZZEGHOUD M., DORBATH L., LEGRAZAND D., DESCHAMPS A., RIVERA L. & BENHALLOU H. (2003). -
912 Seismic source study of the 1989, October 29, Chenoua (Algeria) earthquake from aftershocks, broad-band and
913 strong ground motion records. - *Ann. Geophys.*, **46**, 625–646.
- 914 BOURGOIS J., MAUFFRET A., AMMAR A. & DEMNATI A. (1992). - Multichannel seismic data imaging of inversion
915 tectonics of the Alboran ridge (western Mediterranean Sea). - *Geo-Mar. Lett.*, **12**, 117-122.
- 916 BUFORN E., UDÍAS A. & MEZCUA J. (1988). - Seismicity and focal mechanisms in south Spain. - *Bull. Seism. Soc. Am.*,
917 **78**, 2008–2024.
- 918 BUFORN E., SANZ DE GALDEANO C. & UDÍAS A. (1995). - Seismotectonics of Ibero–Maghrebian region. -
919 *Tectonophysics*, **248**, 247-261.
- 920 BUFORN E., BEZZEGHOUD M., UDÍAS A. & PRO C. (2004). - Seismic sources on the Iberia-African plate boundary and
921 their tectonic implications. - *Pure Appl. Geophys.*, **161**, 623-646.
- 922 BURG J.-P. & CHEN G.M. (1984). - Tectonics and structural zonation of southern Tibet, China. - *Nature*, **311**, 219-223.
- 923 BURRUS J. (1984). - Contribution to a geodynamic synthesis of the Provençal basin (north-western Mediterranean). -
924 *Mar. Geol.*, **55**, 247-269.
- 925 CABY R., HAMMOR D. & DELOR C. (2001). - Metamorphic evolution, partial melting and Miocene exhumation of lower
926 crust in the Edough metamorphic core complex, west Mediterranean orogen, eastern Algeria. - *Tectonophysics*,
927 **342**, 239-273.
- 928 CADET J.-P. & FUNICIELLO R., Eds., (2004). - Geodynamic map of the Mediterranean. Sheet 2, Seismicity and
929 Tectonics. - Commission for the Geological Map of the World, Centre Impression, Limoges, France.
- 930 CALAIS E., NOCQUET J.M., JOUANNE F. & TARDY M. (2002). - Current strain regime in the Western Alps from
931 continuous Global Positioning System measurements, 1996–2001. - *Geology*, **30**, 651–654.
- 932 CALVERT A., GOMEZ F., SEBER D., BARAZANGI M., JABOUR N., IBENBRAHIM A. & DEMNATI A. (1997). - An integrated
933 geophysical investigation of recent seismicity in the Al Hoceima Region of North Morocco. - *Bull. Seismol. Soc.*
934 *Am.*, **87**, 637–651.
- 935 CALVERT A., SANDVOL E., SEBER D., BARAZANGI M., ROECKER S., MOURABIT T., VIDAL F., ALGUACIL G. & JABOUR N.
936 (2000). - Geodynamic evolution of the lithosphere and upper mantle beneath the Alboran region of the western
937 Mediterranean: constraints from travel time tomography. - *J. Geophys. Res.*, **105**, 10871–10898.
- 938 CAMPOS J., MALDONADO A. & CAMPILLO A.C. (1992). - Post-Messinian evolutionary patterns of the central Alboran
939 Sea. - *Geo-Mar. Lett.*, **12**, 173-178.
- 940 CARMINATI E., WORTEL R., MEIJER P.TH. & SABADINI R. (1998). - The two-stage opening of the western-central
941 Mediterranean basins: a forward modeling test to a new evolutionary model. - *Earth Planet. Sc. Lett.*, **160**, 667-
942 679.
- 943 CARMINATI E., WORTEL R., SPAKMAN W. & SABADINI R. (1998). - The role of slab-detachment processes in the
944 opening of the western-central Mediterranean basins: some geological and geophysical evidence. - *Earth Planet.*
945 *Sc. Lett.*, **160**, 651-665.
- 946 CARMINATI E., LUSTRINO M., CUFFARO M. & DOGLIONI C. (2010). - Tectonics, magmatism and geodynamics of Italy:
947 What we know and what we imagine. *J. Virt. Expl.*, **36**, paper 8.
- 948 CATALANO R., FRANCHINO A., MERLINI S. & SULLI A. (2000). - A crustal section from the Eastern Algerian basin to the
949 Ionian ocean (Central Mediterranean). - *Mem. Soc. Geol. Ital.*, **55**, 71–85.
- 950 CHAMOOT-ROOKE N., GAULIER J.M. & JESTIN F. (1999). - Constraints on Moho depth and crustal thickness in the
951 Liguro-Provençal basin from 3D gravity inversion: geodynamic implications. In: Durand, B., *et al.* (Ed.), In
952 the Mediterranean Basins: Tertiary Extension within the Alpine Orogen. Geological Society of London Special
953 Publication, vol. 156, pp. 37–62.
- 954 CHAMPION C., CHOUKROUNE P. & CLAUZON G. (2000). - La déformation post-Miocène en Provence occidentale. -
955 *Geodin. Acta*, **13**, 67-95.
- 956 CHARDON C. & BELLIER O. (2003). - Geological boundary conditions of the 1909 Lambesc (Provence, France)
957 earthquake: structure and evolution of the Trévaresse ridge anticline. *Bull. Soc. géol. France*, **174**, 497-510.
- 958 CHARDON D., HERMITTE D., NGUYEN F. & BELLIER O. (2005). - First paleoseismological constraints on the strongest
959 earthquake in France (Provence) in the Twentieth Century. - *Geology*, **33**, 901-904.
- 960 CHERCHI A. & MONTANDERT L. (1982). - Oligo-Miocene rift of Sardinia and the early history of the western
961 Mediterranean basin. - *Nature*, **298**, 736-739.
- 962 CHEVAL F., DAUTRIA J.-M. & GIROD M. (1989). - Les enclaves de lherzolite à grenat et spinelle du volcan burdigalien
963 de Beaulieu (Bouches-du-Rhône) : des témoins d'une remontée du manteau supérieur associée à l'ouverture du
964 bassin océanique provençal. - *C. R. Acad. Sci. Paris*, **309**, 1309-1315.
- 965 CHIARABBA C., JOVANE L. & DI STEFANO R. (2005). - A new look to the Italian seismicity: Seismotectonic inference.
966 *Tectonophysics*, **395**, 251-268.
- 967 CLOETHING S., GRADSTEIN F.M., KOOI H., GRANT A.C. & KAMINSKI M. (1990). - Plate reorganisation: A cause of rapid
968 late Neogene subsidence and sedimentation around the North Atlantic? - *J. Geol. Soc. London*, **147**, 495-506.

- 969 CLOETINGH S. & KOOI H. (1992). - Tectonics and global change – Inferences from late Cenozoic subsidence and uplift
970 patterns in the Atlantic Mediterranean region. - *Terra Nova*, **4**, 340-350.
- 971 CLOETINGH S.A.P.L., WORTEL M.J.R., & VLAAR N.J. (1982). – Evolution of passive continental margins and initiation
972 of subduction zones. - *Nature*, **297**, 139-142.
- 973 CLOOS M. (1993). – Lithospheric buoyancy and collisional orogenesis: subduction of oceanic plateaus, continental
974 margins, island arcs, spreading ridges, and seamounts. - *Geol. Soc. Am. Bull.*, **105**, 715-737.
- 975 COMAS M.C., GARCÍA-DUEÑAS V. & JURADO M.J. (1992). - Neogene extensional tectonic evolution of the Alboran
976 Basin from MSC data. - *Geo-Mar. Lett.*, **12**, 157– 164.
- 977 COMAS M.C., DAÑOBEITIA J.J., ALVAREZ-MARRON J. & SOTO J.L. (1997). – Crustal reflections and structure in the
978 Alboran Basin: preliminary results of the ESCI-Alboran Survey. - *Rev. Soc. Geol. Espanha*, **8**, 529-542.
- 979 COMAS M.C., PLATT J.P., SOTO J.I. & WATTS A.B. (1999). - The origin and tectonic history of the Alboran Basin:
980 Insights from Leg 161 results. *Proc. Ocean Drill. Program Sci. Results*, **161**, 555– 580.
- 981 CORRADO S., ALDEGA L., BALESTRIERI M.L., MANISCALCO R. & GRASSO M. (2009). - Structural evolution of the
982 sedimentary accretionary wedge of the alpine system in eastern Sicily: Thermal and thermochronological
983 constraints. - *Geol. Soc. Am. Bull.*, **121**, 1475-1490.
- 984 COULON C., MEGARTSI M., FOURCADE S., MAURY R.C., BELLON H., LOUNI-HACINI A., COTTON J., COUTELLE A. &
985 HERMITTE D. (2002). - Post-collisional transition from calc-alkaline to alkaline volcanism during the Neogene in
986 Oranie (Algeria): Magmatic expression of a slab breakoff. *Lithos*, **62**, 87-110.
- 987 CUSHING E.M., BELLIER O., NECHTSCHIEIN S., SÉBRIER M., LOMAX A., VOLANT PH., DERVIN P., GUIGNARD P. & BOVE
988 L. (2008). - A multidisciplinary study of a slow-slipping fault for seismic hazard assessment: the example of the
989 Middle Durance Fault (SE France). - *Geophys. J. Int.*, **172**, 1163-1178.
- 990 D'AGOSTINO N. & SELVAGGI G. (2004). - Crustal motion along the Eurasia-Nubia plate boundary in the Calabrian Arc
991 and Sicily and active extension in the Messina Straits from GPS measurements. - *J. Geophys. Res.*, **109**, B11402,
992 doi:10.1029/2004JB002998.
- 993 D'AGOSTINO N., AVALLONE A., CHELONI D., D'ANASTASIO E., MANTENUTO S. & SELVAGGI G. (2008). - Active
994 tectonics of the Adriatic region from GPS and earthquake slip vectors. - *J. Geophys. Res.*, **113**, B12413, doi:
995 10.1029/2008JB005860.
- 996 DELACOU B., SUE C., NOCQUET J.-M., CHAMPAGNAC J.-D., ALLANIC C. & BURKHARD M. (2008). – Quantification of
997 strain rate in the Western Alps using geodesy: comparisons with seismotectonics. – *Swiss J. Geosci.*, **101**, 377-
998 385.
- 999 DERCOURT J., ZONENSHAIN L.P., RICOU L.-E., KAZMIN V.G., LE PICHON X., KNIPPER A.L., GRANDJACQUET C.,
1000 SBORTSHIKOV I.M., GEYSSANT J., LEPVRIER C., PECHERSKY D.H., BOULIN J., SIBUET J.-C., SAVOSTIN L.A.,
1001 SOROKHTIN O., WESTPHAL M., BAZHENOV M.L., LAUER J.P. & BIJU-DUVAL B. (1986). - Geological evolution of
1002 the Tethys belt from the Atlantic to the Pamirs since the Lias. - *Tectonophysics*, **123**, 241-315.
- 1003 DESSA J.-X., SIMON S., LELIÈVRE M., BESLIER M.-O., DESCHAMPS A., BÉTHOUX N., SOLARINO S., SAGE F., EVA E.,
1004 FERRETTI G., BELLIER O., & EVA C. (2011). – The GROSmarin experiment: three dimensional crustal structure of
1005 the north Ligurian margin from refraction tomography and preliminary analysis of microseismic measurements.
1006 *Bull. Soc. géol. France*, this issue.
- 1007 DÉVERCHÈRE J., YELLES K., DOMZIG A., MERCIER DE LÉPINAY B., BOUILLIN J.-P., GAULLIER V., BRACÈNE R., CALAIS
1008 E., SAVOYE B., KHERROUBI A., LE ROY P., PAUC H. & DAN G. (2005). - Active thrust faulting offshore
1009 Boumerdes, Algeria, and its relations to the 2003 Mw 6.9 earthquake. - *Geophys. Res. Lett.*, **32**, L04311,
1010 doi:10.1029/2004GL021646.
- 1011 DÉVERCHÈRE D., MERCIER DE LÉPINAY B., CATTANEO A., STRZERZYNSKI P., CALAIS E., DOMZIG A. & BRACÈNE R.
1012 (2010). - Comment on “Zemmouri earthquake rupture zone (Mw 6.8, Algeria): Aftershocks sequence relocation
1013 and 3D velocity model” by A. Ayadi et al. - *J. Geophys. Res.*, **115**, B04319, doi:10.1029/2008JB006190.
- 1014 DEWEY J.F., HELMAN M.L., TURCO E., HUTTON D.H.W. & KNOTT D. (1989). - Kinematics of the western
1015 Mediterranean. In: COWARD M.P., DIETRICH D., PARK R.G., Eds., *Alpine Tectonics*. - *Geol. Soc. Spec. Publ.*, **45**,
1016 265-283.
- 1017 DOCHERTY C. & BANDA E. (1995). - Evidence for eastward migration of the Alboran Sea based on regional subsidence
1018 analysis: A case for basin formation by delamination of the subcrustal lithosphere? - *Tectonics*, **14**, 804-818.
- 1019 DOGLIONI C. (1991). – A proposal for the kinematic modelling of W-dipping subductions – Possible applications to the
1020 Tyrrhenian Apennines system. – *Terra Nova*, **3**, 423-434.
- 1021 DOGLIONI C., GUEGUEN E., SABAT F. & FERNANDEZ M. (1997). - The western Mediterranean extensional basins and the
1022 Alpine orogen. - *Terra Nova*, **9**, 109-112.
- 1023 DOGLIONI C., INNOCENTI F. & MARIOTTI G. (2001). - Why Mt Etna? - *Terra Nova*, **13**, 25-31.
- 1024 DOGLIONI C., CARMINATI E., CUFFARO M. & SCROCCA D. (2007). – Subduction kinematics and dynamic constraints.
1025 *Earth-Sc. Rev.*, **232**, 125-175.
- 1026 DOMZIG A., YELLES K., LE ROY C., DÉVERCHÈRE J., BOUILLIN J.-P., BRACÈNE R., MERCIER DE LÉPINAY B., LE ROY P.,
1027 CALASI E., KHERROUBI A., GAULLIER V., SAVOYE B. & PAUC H. (2006). - Searching for the Africa-Eurasia
1028 Miocene boundary offshore western Algeria (MARADJA'03 cruise). - *C. R. Geosci.*, **338**, 80–91.

- 1029 DUGGEN S., HOERNLE K., VAN DEN BOGAARD, P. & HARRIS C. (2004). - Magmatic evolution of the Alboran Region: the
1030 role of subduction in forming the western Mediterranean and causing the Messinian Salinity Crisis. *Earth Planet.
1031 Sc. Lett.*, **218**, 91–108.
- 1032 DUGGEN S., HOERNLE K., VAN DEN BOGAARD, P. & GARBE-SCHÖNBERG D. (2005). – Post-collisional transition from
1033 subduction-to intraplate-type magmatism in the westernmost Mediterranean: evidence fro continental-edge
1034 delamination of subcontinental lithosphere. – *J. Petrol.*, **46**, 1155-1201.
- 1035 DUTOUR A., PHILIP H., JAURAND E. & COMBES P. (2002). - Mise en evidence de déformations en faille inverse avec
1036 ruptures de surface cosismiques dans des depots colluviaux wurmiens du versant nord du mont Ventoux
1037 (Provence occidentale, France). - *C. R. Geosci.*, **334**, 849–856.
- 1038 DZIEWONSKI A.M., CHOU T.-A. & WOODHOUSE J.H. (1981) – Determination of earthquake source parameters from
1039 waveform data for studies of global and regional seismicity. - *J. Geophys. Res.*, **86**, 2825–2852.
- 1040 DZIEWONSKI A.M., EKSTRÖM G. & MATERNOVSKAYA N.N. (2000). - Centroid–moment tensor solutions for October–
1041 December, 1999. - *Phys. Earth Planet. Int.*, **121**, 205-221.
- 1042 EL MRABET T. (2005). - The great earthquakes in the Maghreb region and their consequences on man and environment
1043 (in Arabic with abstract in English). - Edit. Centre National de Recherche Scientifique et Technique, Rabat,
1044 Morocco.
- 1045 ERICKSON S.G. & ARKANI-HAMED J. (1993). - Subduction initiation at passive margins: The Scotian basin, eastern
1046 Canada as a potential example. - *Tectonics*, **12**, 678–687.
- 1047 ESCAYOLA M.P., PIMENTEL M.M. & ARMSTRONG R. (2007). - Neoproterozoic backarc basin: Sensitive high-resolution
1048 ion microprobe U-Pb and Sm-Nd isotopic evidence from the Eastern Pampean Ranges, Argentina. - *Geology*, **35**,
1049 495-498.
- 1050 EVA E., SOLARINO S. & SPALLAROSSA D. (2001). – Seismicity and crustal structure beneath the western Ligurian Sea
1051 derived from local earthquake tomography. – *Tectonophysics*, **339**, 495-510.
- 1052 FACCENNA C., MATTEI M., FUNICIELLO R. & JOLIVET L. (1997). - Styles of back-arc extension in the central
1053 Mediterranean. - *Terra Nova*, **9**, 126-130.
- 1054 FACCENNA C., GIARDINI D., DAVY P. & ARGENTIERI A. (1999). - Initiation of subduction at Atlantic-type margins:
1055 Insights from laboratory experiments, *J. Geophys. Res.*, **104**, 2749-2766.
- 1056 FACCENNA C., FUNICIELLO F., GIARDINI D. & LUCENTE P.,(2001). - Episodic back-arc extension during restricted
1057 mantle convection in the Central Mediterranean. - *Earth Planet. Sci. Lett.*, **187**, 105-116.
- 1058 FACCENNA C., SPERANZA F., D'AJELLO CARACCILO F., MATTEI M. & OGGIANO G. (2002). - Extensional tectonics on
1059 Sardinia (Italy): insights into the arc–back-arc transitional regime. *Tectonophysics*, **356**, 213–232.
- 1060 FACCENNA C., PIROMALLO C., CRESPO-BLANC A. & JOLIVET L. (2004). - Lateral slab deformation and the origin of the
1061 western Mediterranean arcs. - *Tectonics*, **23**, TC1012, doi:10.1029/2002TC001488.
- 1062 FACCENNA C., CIVETTA L., D'ANTONIO M., FUNICIELLO F., MARGHERITI L. & PIROMALLO C. (2005). – Constraints on
1063 mantle circulation around the deforming Calabrian slab. - *Geophys. Res. Lett.*, **32**, L06311,
1064 doi:10.1029/2004GL021874.
- 1065 FACCENNA C., MOLIN P., ORECCHIO B., OLIVETTI V., BELLIER O., FUNICIELLO F., MINELLI L., PIROMALLO C. & BILLI A.
1066 (2011). - Topography of the Calabria subduction zone (southern Italy): clues for the origin of Mt Etna. -
1067 *Tectonics*, doi:10.1029/2010TC002694, in press.
- 1068 FERNÁNDEZ-IBÁÑEZ F., SOTO J.I., ZOBACK M.D. & MORALES J. (2007). – Present-day stress field in the Gibraltar Arc
1069 (western Mediterranean). - *J. Geophys. Res.*, **112**, B08404, doi:10.1029/2006JB004683.
- 1070 FERRARI G. (1991). - The 1887 Ligurian earthquake: a detailed study from contemporary scientific observations. –
1071 *Tectonophysics*, **193**, 131–139.
- 1072 FOURCADE S., CAPIDEVILLA R., OUBADI A. & MARTINEAU F. (2001). - The origin and geodynamic significance of the
1073 Alpine cordierite-bearing granitoids of northern Algeria: A combined petrological, mineralogical, geochemical
1074 and isotopic (O, H, Sr, Nd) study. - *Lithos*, **57**, 187-216.
- 1075 FRIZON DE LAMOTTE D., SAINT BEZAR B., BRACÈNE R. & MERCIER E. (2000). - The two main steps of the Atlas
1076 building and geodynamics of the western Mediterranean. - *Tectonics*, **19**, 740-761.
- 1077 GATTACCECA J., DEINO A., RIZZO R., JONES D.S., HENRY B., BEAUDOIN B. & VADEBOIN F. (2007). -Miocene rotation of
1078 Sardinia: new paleomagnetic and geochronological constraints and geodynamic implications. *Earth Planet. Sc.
1079 Lett.*, **258**, 359–377.
- 1080 GHISETTI, F. (1979). - Relazioni tra strutture e fasi trascorrenti e distensive lungo i sistemi Messina-Fiumefreddo,
1081 Tindari-Letojanni e Alia-Malvagna (Sicilia nord-orientale): Uno studio micro tettonico. *Geol. Romana*, **18**, 23-
1082 58.
- 1083 GHISETTI F., GORMAN A.R., GRASSO M. & VEZZANI L. (2009). – Imprint of foreland structure on the deformation of a
1084 thrust sheet: the Plio-Pleistocene Gela Nappe (southern Sicily, Italy). - *Tectonics*, **28**, TC4015,
1085 doi:10.1029/2008TC002385.
- 1086 GIARDINI D., BOSCHI E. MAZZA S., MORELLI A., BEN SARI D., NAJID D., BENHALLOU H., BEZZEGHOUD M., TRABELSI
1087 H., HFAIDH M., KEBEASY R.M. AND IBRAHIM E.M. (1992) - Very-broad-band seismology in Northern Africa
1088 under the MedNet project, *Tectonophysics*, 209, 17-30.
- 1089 GOES S., GIARDINI D., JENNY S., HOLLENSTEIN C., KAHLE H.G. & GEIGER A. (2004). - A recent tectonic reorganization
1090 in the south-central Mediterranean. - *Earth Planet. Sci. Lett.*, **226**, 335-345.

- 1091 GOMEZ F.W., ALLMENDINGER R., BARAZANGI M., ER-RAJI A. & DAHMANI M. (1998). - Crustal shortening and vertical
1092 strain partitioning in the Middle Atlas Mountains of Morocco. - *Tectonics*, **17**, 520-533.
- 1093 GORINI C., MAUFFRET A., GUENOC P. & LE MARREC A. (1994). - Structure of the Gulf of Lions (northwestern
1094 Mediterranean Sea): A review. In: MASCLE A., Ed., Hydrocarbon and Petroleum Geology of France. Eur. Assoc.
1095 of Pet. Geol., pp. 223-243, Houten, Netherlands.
- 1096 GOVERS R. & WORTEL M.J.R. (2005). - Lithosphere tearing at STEP faults: response to edges of subduction zones. -
1097 *Earth Planet. Sci. Lett.*, **236**, 505-523.
- 1098 GRÀCIA E., PALLÀS R., SOTO J.I., COMAS M.C., MORENO X., MASANA E., SANTANACH P., DIEZ S., GARCÍA M.,
1099 DAÑOBEITIA J.J. & HITS SCIENTIFIC PARTY (2006). - Active faulting offshore SE Spain (Alboran Sea):
1100 Implications for earthquake hazard assessment in the southern Iberian Margin. - *Earth Planet. Sci. Lett.*, **241**,
1101 734– 749.
- 1102 GUEGUEN E., DOGLIONI C. & FERNANDEZ M. (1997). - Lithospheric boudinage in the Western Mediterranean back-arc
1103 basins. - *Terra Nova*, **9**, 184-187.
- 1104 GUEGUEN E., DOGLIONI C. & FERNANDEZ M. (1998). - On the post-25 Ma geodynamic evolution of the Western
1105 Mediterranean. - *Tectonophysics*, **298**, 259-269.
- 1106 GUIGNARD P., BELLIER O. & CHARDON D. (2005). Géométrie et cinématique post-oligocène des Failles d'Aix et de la
1107 Moyenne Durance (Provence, France). - *C.R. Géoscience, Acad. Sc. Paris*, **337/3**, 375-384.
- 1108 GUTSCHER M.A., MALOD J., REHAULT J.P., CONTRUCCI I., KLINGELHOEFER F., MENDES-VICTOR L. & SPAKMAN W.
1109 (2002). - Evidence for active subduction beneath Gibraltar. *Geology*, **30**, 1071–1074.
- 1110 GUTSCHER M.A., DOMINGUEZ S., WESTBROOK G.K., LEROY P. (2009). - Deep structure, recent deformation and analog
1111 modeling of the Gulf of Cadiz accretionary wedge: implications for the 1755 Lisbon earthquake. -
1112 *Tectonophysics*, **475**, 85-97.
- 1113 GVIRTZMAN Z. & NUR A. (1999). - The formation of Mount Etna as the consequence of slab rollback. *Nature*, **401**, 782-
1114 785.
- 1115 HENARES J., LÓPEZ CASADO C., SANZ DE GALDEANO C., DELGADO J. & PELÀEZ J.A. (2003). - Stress fields in the
1116 Iberian-Maghrebian region. - *J. Seismol.*, **7**, 65–78,
- 1117 HERRING T., KING R.W. & MCCLUSKY S. (2006). - GAMIT Reference Manual, Release 10.3. Department of Earth,
1118 Atmospheric, and Planetary Sciences, Massachusetts Institute of Technology.
- 1119 HOLLENSTEIN CH., KAHLE H.-G., GEIGER A., JENNY S., GOES S. & GIARDINI D. (2003). - New GPS constraints on the
1120 Africa-Eurasia plate boundary zone in southern Italy. *Geophys. Res. Lett.*, **30**, 1935, doi:10.1029/2003GL017554.
- 1121 HOUSE M.A., GURNIS M., KAMP P.J.J. & SUTHERLAND R. (2002). - Uplift in the Fiordland region, New Zealand:
1122 Implications for incipient subduction. - *Science*, **297**, 2038–2041, doi:10.1126/science.1075328.
- 1123 HIPPOLYTE J.-C., ANGELIER J., BERGERAT F., NURY D. & GUIEU G. (1993). - Tectonic-stratigraphic record of
1124 paleostress time changes in the Oligocene basins of the Provence, southern France. - *Tectonophysics*, **226**, 15-
1125 35.
- 1126 HIPPOLYTE J.-C. & DUMONT T. (2000). - Identification of Quaternary thrusts, folds and faults in a low seismicity area:
1127 examples in the Southern Alps (France). - *Terra Nova*, **12**, 156-162.
- 1128 JIMÉNEZ-MUNT I., FERNÁNDEZ M., VERGÉS J., AFONSO J.C., GARCIA-CASTELLANOS D. & FULLEA J. (2010). - The
1129 lithospheric structure of the Goringe Bank: insights into its origin and tectonic evolution. - *Tectonics*, **29**,
1130 TC5019, doi:10.1029/2009TC002458.
- 1131 JOLIVET L. & FACCENNA C. (2000). - Mediterranean extension and the Africa-Eurasia collision. - *Tectonics*, **19**, 1095-
1132 1106.
- 1133 JOLIVET L., FACCENNA C., GOFFÉ B., BUROV E. & AGARD P. (2003). - Subduction tectonics and exhumation of high-
1134 pressure metamorphic rocks in the Mediterranean orogens. - *Am. J. Sci.*, **303**, 353-409.
- 1135 JOLIVET L., AUGIER R., FACCENNA C., NEGRO F., RIMMELE G., AGARD P., ROBIN C., ROSSETTI F. & CRESPO-BLANC A.
1136 (2008). - Subduction, convergence and the mode of backarc extension in the Mediterranean region. - *Bull. Soc.
1137 géol. Fr.*, **179**, 525-550.
- 1138 JOLIVET L., FACCENNA C. & PIROMALLO C. (2009). - From mantle to crust: stretching the Mediterranean. - *Earth
1139 Planet. Sc. Lett.*, **285**, 198-209.
- 1140 KASTENS K.A. & MASCLE J. (1990). - The geological evolution of the Tyrrhenian Sea: An introduction to the scientific
1141 results of ODP Leg 107. - *Proc. Ocean Drill. Program Sci. Results*, **107**, 3-26.
- 1142 KASTENS K.A., MASCLE J. & O.L.S. PARTY (1988). - ODP Leg 107 in the Tyrrhenian Sea: Insights into passive margin
1143 and backarc basin evolution. - *Geol. Soc. Am. Bull.*, **100**, 1140-1156.
- 1144 KAPP P., YIN A., MANNING C.E., HARRISON T.M. & TAYLOR M.H. (2003). - Tectonic evolution of the early Mesozoic
1145 blueschist-bearing metamorphic belt, central Tibet. - *Tectonics*, **24**, 1043, doi: 1029/2002TC001383.
- 1146 KHERROUBI A., DÉVERCHÈRE J., YELLES A.K., MERCIER DE LÉPINAY B., DOMZIG A., CATTANEO A., BRACENE R.,
1147 GAULLIER V. & GRAINDORGE D. (2009). - Recent and active deformation pattern off the easternmost Algerian
1148 margin, western Mediterranean Sea: New evidence for contractional tectonic reactivation. - *Mar. Geol.*, **261**, 17–
1149 32.
- 1150 LACASSIN R., TAPPONNIER P., MEYER B. & ARMIJO R. (2001). - Was the Trévaresse Thrust the source of the 1909
1151 Lambesc (Provence, France) earthquake? Historical and geomorphic evidence. - *C.R. Acad. Sci. Paris*, **333**,
1152 571-581.

- 1153 LALLEMAND S., HEURET A., FACCENNA C. & FUNICIELLO F. (2008). - Subduction dynamics as revealed by trench
1154 migration. *Tectonics*, **27**, TC3014, doi:10.1029/2007TC002212.
- 1155 LAMMALI K., BEZZEGHOUD M., OUSSADAU F., DIMITROV D. & BENHALLOU H. (1997). - Potseismic deformation at El
1156 Asnam (Algeria) in the seismotectonic context of northwestern Algeria. *Geophys. J. Int.*, **129**, 597-616.
- 1157 LARROQUE C., BÉTHOUX N., CALAIS E., COURBOULEX F., DESCHAMPS A., DÉVERCHÈRE J., STÉPHAN J.F., RITZ J.F. &
1158 GILLI E. (2001). - Active deformation at the junction between southern French Alps and Ligurian basin. – *Neth.*
1159 *J. Geosc.*, **80**, 255–272.
- 1160 LARROQUE C., DELOUIS B., GODEL B. & NOCQUET J.M. (2009). - Active deformation at the southwestern Alps–Ligurian
1161 basin junction (France–Italy boundary): Evidence for recent change from compression to extension in the
1162 Argentera massif. - *Tectonophysics*, **467**, 22-34.
- 1163 LICKORISH W.H., GRASSO M., BUTLER R.W.H., ARGNANI A. & MANISCALCO R. (1999). - Structural styles and regional
1164 tectonic setting of the “Gela Nappe” and frontal part of the Maghrebian thrust belt in Sicily. - *Tectonics*, **18**, 655-
1165 668, doi:10.1029/1999TC900013.
- 1166 LE PICHON X., PAUTOT G., AUZENDE J.-M., & OLIVET J.-L. (1971). – La Méditerranée occidentale depuis l’Oligocène. –
1167 *Earth Planet. Sci. Lett.*, **13**, 145-152.
- 1168 LONERGAN L. & WHITE N. (1997). - Origin of the Betic-Rif mountain belt. - *Tectonics*, **16**, 504–522.
- 1169 LÓPEZ CASADO C., SANZ DE GALDEANO C., MOLINA PALACIOS C. & HENARES ROMERO J. (2001). – The structure of the
1170 Alboran Sea: an interpretation from seismological and geological data. – *Tectonophysics*, **338**, 79-95.
- 1171 LUSTRINO M., DUGGEN S., & ROSENBERG C.L. (2011). – The Central-Western Mediterranean: anomalous igneous
1172 activity in an anomalous collisional tectonic setting. *Eart-Sc. Rev.*, in press.
- 1173 MAILLARD A. & MAUFFRET A. (1999). - Crustal structure and riftogenesis of the Valencia Trough (northwestern
1174 Mediterranean Sea). - *Basin Res.*, **11**, 357-379.
- 1175 MALINVERNO A. & RYAN W.B.F. (1986). - Extension in the Tyrrhenian Sea and shortening in the Apennines as result of
1176 arc migration driven by sinking of the lithosphere. - *Tectonics*, **5**, 227-254.
- 1177 MARTÍNEZ- MARTÍNEZ J.M., SOTO J.I. & BALANYÁ J.C. (2002). – Orthogonal folding of extensional detachments:
1178 structure and origin of the Sierra Nevada elongated dome (Betics, SE Spain). – *Tectonics*, **21**, 1012,
1179 doi:10.1029/2001TC001283.
- 1180 MASCLE G.H., TRICART P., TORELLI L., BOUILLIN J.P., COMPAGNONI R., DEPARDON S., MASCLE J., PECHER A., PEIS D.,
1181 REKHISS F., ROLFO F., BELLON H., BROCARD G., LAPIERRE H., MONIÉ P. & POUPEAU G. (2004). – Structure of
1182 the Sardinia Channel: crustal thinning and tardi-orogenic extension in the Apenninic-Maghrebian orogen; results
1183 of the Cyana submersible survey (SARCYA and SARTUCYA) in the western Mediterranean. *Bull. Soc. geol.*
1184 *Fr.*, **175**, 607-627.
- 1185 MATTEI M., CIFELLI F. & D’AGOSTINO N. (2007). - The evolution of the Calabrian Arc: Evidence from paleomagnetic
1186 and GPS observations. - *Earth Planet. Sci. Lett.*, **263**, 259-274.
- 1187 MAUFFRET A., MALDONADO A. & CAMPILLO A.C. (1992). – Tectonic framework of the eastern Alboran and western
1188 Algerian basins, western Mediterranean. – *Geo-Mar. Lett.*, **12**, 104-110.
- 1189 MAUFFRET A., FRIZON DE LAMOTTE D., LALLEMANT S., GORINI C. & MAILLARD A. (2004). E–W opening of the
1190 Algerian Basin (Western Mediterranean). - *Terra Nova*, **16**, 257–264.
- 1191 MAUFFRET A. (2007). - The northwestern (Maghreb) boundary of the Nubia (Africa) Plate. - *Tectonophysics*, **429**, 21-
1192 44.
- 1193 MAURY R.C., FOURCADE S., COULON C., EL AZZOUZI M., BELLON H. COUTELLE A., OUABADI A., SEMROUD B.,
1194 MEGARTSI M., COTTON J., BELANTEUR O., LOUNI-HACINI A., PIQUÉ A., CAPDEVILA R., HERNANDEZ J. &
1195 RÉHAULT J.-P. (2000). – Post-collisional Neogene magmatism of the Mediterranean Maghreb margin: A
1196 consequence of slab break off. - *C. R. Acad. Sci. Ser. Ila Sci. Terre Planetes*, **331**, 159–173.
- 1197 MCCAFFREY R. (2008). - Global frequency of magnitude 9 earthquakes. *Geology*, **36**, 263–266.
- 1198 MEGHRAOUI M. (1991). – Blind reverse faulting system associated with the Mont Chenoua-Tipaza earthquake of 29
1199 October 1989 (north-central Algeria). – *Terra Nova*, **3**, 84-93.
- 1200 MEGHRAOUI M., CISTERNAS A. & PHILIP H. (1986). - Seismotectonics of the lower Cheliff basin: structural background
1201 of the El Asnam (Algeria) earthquake. – *Tectonics*, **5**, 809–836.
- 1202 MEGHRAOUI M., MAUCHE S., CHEMAA B., CAKIR Z., AOUDIA A., HARBI A., ALASSET P.J., AYADI A., BOUHADA Y. &
1203 BENHAMOUDA F. (2004). - Coastal uplift and thrust faulting associated with the M=6.8 Zemmouri (Algeria)
1204 earthquake of 21 May 2003. *Geophys. Res. Lett.*, **31**, L19605, doi:10.1029/2004GL020466.
- 1205 MICHARD A., CHALOUAN A., FEINBERG H., GOFFÉ B. & MONTIGNY R. (2002). – How does the Alpine belt end between
1206 Spain and Morocco? - *Bull. Soc. géol. Fr.*, **173**, 3-15.
- 1207 MINELLI L. & FACCENNA C. (2010). - Evolution of the Calabrian Accretionary wedge (Central Mediterranean).
1208 *Tectonics*, **29**, TC4004, doi:10.1029/2009TC002562.
- 1209 MONACO C., MAZZOLI S. & TORTORICI L. (1996). - Active thrust tectonics in western Sicily (southern Italy): the 1968
1210 Belice earthquake sequence. - *Terra Nova*, **8**, 372-381.
- 1211 MONIÉ P., CABY R. & AND MALUSKI H. (1984). - 40Ar/39Ar investigations within the Grande-Kabylie Massif (northern
1212 Algeria): Evidences for its Alpine structuration. - *Eclogae Geol. Helv.*, **77**, 115–141.
- 1213 MONIÉ P., MALUSKI H., SAADALLAH A. & CABY R. (1988). - New 40Ar/39Ar ages of Hercynian and alpine
1214 thermotectonic events in Grande Kabylie (Algeria). - *Tectonophysics*, **152**, 53-69.

- 1215 MONTONE P., MARIUCCI M.T., PONDRELLI S. & AMATO A. (2004). - An improved stress map for Italy and surrounding
1216 regions (central Mediterranean). - *J. Geophys. Res.*, **109**, B10410, doi:10.1029/2003JB002703.
- 1217 MOREL J.L. & MEGHRAOUI M. (1996). - Goringe-Alboran-Tell tectonic zone: a transpression system along the Africa-
1218 Eurasia plate boundary. - *Geology*, **24**, 755-758.
- 1219 MORELLI A. & DZIEWONSKI A. (1993). - Body wave traveltimes and aspherically symmetric P- and S-wave velocity
1220 model. *Geophys. J. Int.*, **112**, 178-194.
- 1221 MURPHY M.A. & YIN A. (2003). - Structural evolution and sequence of thrusting in the Tethyan fold-thrust belt and
1222 Indus-Yalu suture zone, southwest Tibet. - *Geol. Soc. Am. Bull.*, **115**, 21-34.
- 1223 NERI G., ORECCHIO B., TOTARO C., FALCONE G. & PRESTI D. (2009). - Seismic tomography says that lithospheric
1224 subduction beneath South Italy is close to die. - *Seismol. Res. Lett.*, **80**, 63-70.
- 1225 NGUYEN F., GARAMBOIS S., CHARDON D., JONGMANS D., BELLIER O. & HERMITTE D. (2002). - Etude de failles actives
1226 par méthodes géophysiques combinées : exemple de la Trévaresse. - *Journées AGAP Qualité*, Nantes.
- 1227 NICOLOSI I., SPERANZA F. & CHIAPPINI M. (2006). - Ultrafast oceanic spreading of the Marsili Basin, southern
1228 Tyrrhenian Sea: Evidence from magnetic anomaly analysis. - *Geology*, **34**, 717-720.
- 1229 NOCQUET J.M. & CALAIS E. (2004). - Geodetic measurements of crustal deformation in the Western Mediterranean and
1230 Europe. - *Pure Appl. Geophys.*, **161**, 661-681.
- 1231 NOCQUET J.-M., WILLIS P. & GARCIA S. (2006). - Plate kinematics of Nubia-Somalia using a combined DORIS and
1232 GPS solution. - *J. Geod.*, **80**, 591-607.
- 1233 OUTTAMI F., ADDOUM B., MECIER E., FRIZON DE LAMOTTE D. & ANDRIEUX J. (1995). - Geometry and kinematics of the
1234 south Atlas front, Algeria and Tunisia. - *Tectonophysics*, **249**, 233-248.
- 1235 PATACCA E., SARTORI R. & SCANDONE P. (1992). - Tyrrhenian basin and Apenninic arcs: Kinematic relations since late
1236 Tortonian times. - *Mem. Soc. Geol. It.*, **45**, 425-451.
- 1237 PEÑAA, A.P., MARTÍN-DAVILAB, J., GÁRATEB, J., BERROCOSOA, M. & BUFORNE E. (2010). - Velocity field and tectonic
1238 strain in Southern Spain and surrounding areas derived from GPS episodic measurements. *J. Geod.*, **49**, 232-240.
- 1239 PEPE F., BERTOTTI G., CELLA F. & MARSELLA E. (2000). - Rifted margin formation in the south Tyrrhenian Sea: A high-
1240 resolution seismic profile across the north Sicily passive continental margin. - *Tectonics*, **19**, 241-257.
- 1241 PEPE F., SULLI A., BERTOTTI G. & CATALANO R. (2005). - Structural highs formation and their relationship to
1242 sedimentary basins in the north Sicily continental margin (southern Tyrrhenian Sea): Implication for the Drepano
1243 Thrust Front. *Tectonophysics*, **409**, 1-18.
- 1244 PEPE F., SULLI A., BERTOTTI G. & CELLA F. (2010). - The architecture and Neogene to Recent evolution of the W
1245 Calabrian continental margin: an upper plate perspective to the Ionian subduction system (Central
1246 Mediterranean). - *Tectonics*, doi:10.1029/2009TC002599.
- 1247 PESQUER D.A., GREVENMEYER I., RANERO C.R. & GALLART J. (2008). - Seismic structure of the passive continental
1248 margin of SE Spain and the SW Balearic promontory, western Mediterranean Sea. - *Eos Trans. AGU*, **89**(53),
1249 Fall Meet. Suppl., Abstract 1340H.
- 1250 PHILIP H. & MEGHRAOUI M. (1983). - Structural analysis and interpretation of the surface deformations of the El Asnam
1251 earthquake of October 10, 1980. - *Tectonics*, **2**, 17-49.
- 1252 PIROMALLO C., VINCENT A.P., YUEN D.A. & MORELLI A. (2001). - Dynamics of the transition zone under Europe
1253 inferred from wavelet cross-spectra of seismic tomography. - *Phys. Earth Planet. Inter.*, **125**, 125-139.
- 1254 PIROMALLO C. & MORELLI A. (2003). - P wave tomography of the mantle under the Alpine-Mediterranean area. - *J.*
1255 *Geophys. Res.*, **108**, 2065, doi:10.1029/2002JB001757.
- 1256 PIROMALLO C. & FACCENNA C. (2004). - How deep can we find the traces of Alpine subduction? - *Geophys. Res. Lett.*,
1257 **31**, L06605, doi:10.1029/2003GL019288.
- 1258 PLATT J.P., SOTO J.I., WHITEHOUSE M.J., HURFORD A.J. & KELLEY S.P. (1998). - Thermal evolution, rate of
1259 exhumation, and tectonic significance of metamorphic rocks from the floor of the Alboran extensional basin,
1260 western Mediterranean. - *Tectonics*, **17**, 671-689.
- 1261 PLATT J.P., ALLERTON S., KIRKER A., MANDEVILLE C., MAYFIELD A., PLATZMAN E.S. & RIMI A. (2003). - The ultimate
1262 arc: Differential displacement, oroclinal bending, and vertical axis rotation in the External Betic-Rif arc. -
1263 *Tectonics*, **22**, 1017, doi:10.1029/2001TC001321.
- 1264 POLONIA A., TORELLI L., CAPOZZI R., RIMINUCCI F., ARTONI A., RAMELLA R. & THE CALARC GROUP (2008). -
1265 African/Eurasian plate boundary in the Ionian Sea: shortening and strike slip deformation in the outer
1266 accretionary wedge. GNGTS Meeting, Trieste, October 2008.
- 1267 PONDRELLI S., MORELLI A., EKSTRÖM G., MAZZA S., BOSCHI E. & DZIEWONSKI A.M. (2002). - European-Mediterranean
1268 regional centroid-moment tensors: 1997-2000. - *Phys. Earth Planet. Int.*, **130**, 71-101.
- 1269 PONDRELLI S., MORELLI A. & EKSTRÖM G. (2004). - European-Mediterranean Regional Centroid Moment Tensor
1270 catalog: solutions for years 2001 and 2002. - *Phys. Earth Planet. Int.*, **145**, 127-147.
- 1271 PONDRELLI S., PIROMALLO C. & SERPELLONI E. (2004). - Convergence vs. retreat in southern Tyrrhenian Sea: Insights
1272 from kinematics. - *Geophys. Res. Lett.*, **31**, L06611, doi:10.1029/2003GL019223.
- 1273 PONDRELLI S., SALIMBENI S., EKSTRÖM G., MORELLI A., GASPERINI P. & VANNUCCI G. (2006). - The Italian CMT
1274 dataset from 1977 to the present. - *Phys. Earth Planet. Int.*, **159**, 286-303.
- 1275 PONDRELLI S., MORELLI A., EKSTRÖM G. & BOSCHI E. (2007). - European-Mediterranean Regional Centroid Moment
1276 Tensor catalog: Solutions for years 2003 and 2004. - *Phys. Earth Planet. Int.*, **164**, 90-112.

- 1277 REGARD V., FACCENNA C., BELLIER O. & MARTINOD J. (2008). – Laboratori experiments of slab break-off and slab dip
1278 reversal: insight into the Alpine Oligocene reorganization. – *Terra Nova*, **20**, 267-273.
- 1279 REHAULT J.P. (1981). – Evolution tectonique et sédimentaire du bassin ligure (Méditerranée occidentale). –Thèse
1280 d'Etat, Paris VI, 128 p.
- 1281 RÉHAULT J.P., BOILLOT G. & MAUFFRET A. (1984). - The western Mediterranean Basin geological evolution. - *Mar.*
1282 *Geol.*, **55**, 447-477.
- 1283 RICOU L.E., DERCOURT J., GEYSSANT J., GRANDJACQUET C., LEPVRIER C. & BIJU-DUVAL B. (1986). -Geological
1284 constraints on the alpine evolution of the Mediterranean Tethys. *Tectonophysics*, **123**, 83-122.
- 1285 ROCA E., FRIZON DE LAMOTTE D., MAUFFRET A., BRACENE R., VERGES J., BENAOUALI N., FERNANDEZ M., MUÑOZ J.A.
1286 & ZEYEN H. (2004). - TRANSMED transect II. In: CAVAZZA W., ROURE F.M., SPAKMAN W., STAMPFLI G.M. &
1287 ZIEGLER P.A., Eds., The TRANSMED Atlas. pp. 1–141, Springer, Berlin.
- 1288 RODRÍGUEZ-FERNÁNDEZ J. & SANZ DE GALDEANO C. (2006). – Late orogenic intramontane basin development: the
1289 Granada basin, Betics (southern Spain). *Basin Res.*, **18**, 85-102.
- 1290 ROLLET N., DÉVERCHÈRE J., BESLIER M.O., GUENOC P., RÉHAULT J.P., SOSSON M. & TRUFFERT C., (2002). - Back arc
1291 extension, tectonic inheritance and volcanism in the Ligurian Sea, Western Mediterranean. – *Tectonics*, **21**, 1015,
1292 doi:10.1029/2001TC900027.
- 1293 ROSENBAUM G. & LISTER G.S. (2004). - Neogene and Quaternary rollback evolution of the Tyrrhenian Sea, the
1294 Apennines, and the Sicilian Maghrebides. - *Tectonics*, **23**, TC1013, doi:10.1029/2003TC001518.
- 1295 ROSENBAUM G., LISTER G.S. & DUBOZ C. (2002). - Relative motions of Africa, Iberia and Europe during Alpine
1296 orogeny. *Tectonophysics*, **359**, 117-129.
- 1297 ROSSETTI F., FACCENNA C., GOFFÉ B., MONIÉ P., ARGENTIERI A., FUNICIELLO R. & MATTEI M. (2001). - Alpine
1298 structural and metamorphic signature of the Sila Piccola Massif nappe stack (Calabria, Italy): Insights for the
1299 tectonic evolution of the Calabrian Arc. - *Tectonics*, **20**, 112-133.
- 1300 ROSSETTI R., GOFFÉ B., MONIÉ P., FACCENNA C. & VIGNAROLI G. (2004). - Alpine orogenic P-T-t-deformation history
1301 of the Catena Costiera area and surrounding regions (Calabrian Arc, southern Italy): The nappe edifice of north
1302 Calabria revised with insights on the Tyrrhenian-Apennine system formation. - *Tectonics*, **23**,
1303 doi:10.1029/2003TC001560.
- 1304 ROSSETTI F., THEYE T., LUCCI F., BOUYBAOUENE M.L., DINI A., GERDES A., PHILLIPS D. & COZZUPOLI D. (2010). -
1305 Timing and modes of granite magmatism in the core of the Alboran Domain, Rif chain, northern Morocco:
1306 Implications for the Alpine evolution of the western Mediterranean. - *Tectonics*, **29**, TC2017,
1307 doi:10.1029/2009TC002487.
- 1308 ROTHE J.P. (1950). - Les séismes de Kherrata et la sismicité de l'Algérie. - *Bull. Serv. Carte Geol. Alger. Ser. 4*, **3**, 3–
1309 40.
- 1310 ROURE F., CASERO P. & VIALLY R. (1991). - Growth process and melange formation in the southern Apennines
1311 accretionary wedge. - *Earth Planet. Sci. Lett.*, **102**, 395-412.
- 1312 ROYDEN L.H. (1993). - Evolution of retreating subduction boundaries formed during continental collision. - *Tectonics*,
1313 **12**, 629-638.
- 1314 SAADALLAH A. & CABY, R. (1996). - Alpine extensional detachment tectonics in the Grande Kabylie metamorphic core
1315 complex of the Maghrebides (northern Algeria). – *Tectonophysics*, **267**, 257–273.
- 1316 SAADALLAH A., BELHAI D., DJELLIT H. & SEDDIK N. (1996). - Dextral fault motion between the internal and external
1317 zones of the Maghrebides, and flower structure in the Limestone Range, Djurdjura Massif, Algeria. - *Geodin.*
1318 *Acta*, **9**, 177–188.
- 1319 SANCHEZ G., ROLLAND Y., SCHREIBER D., GIANNERINI G., CORSINI M. & LARDEAUX J.-M. (2010). – The active fault
1320 system of SW Alps. – *J. Geodyn.*, **49**, 296-302.
- 1321 SARTORI R. (1990). - The main results of ODP Leg 107 in the frame of Neogene to recent geology of peri-Tyrrhenian
1322 areas. - *Proc. Ocean Drill. Program Sci. Results*, **107**, 715-730.
- 1323 SCETTINO A. & TURCO E. (2006). - Plate kinematics of the western Mediterranean region during the Oligocene and
1324 Early Miocene. - *Geophys. J. Int.*, **166**, 1398–1423,
- 1325 SCROCCA D., DOGLIONI C., INNOCENTI F., MANETTI P., MAZZOTTI A., BERTELLI L., BURBI L. & D'OFFIZI S. (EDS.)
1326 (2003). – CROP Atlas: seismic reflection profiles of the Italian crust. - *Mem. Descr. Carta Geol. It.*, **62**, 194 pp.,
1327 71 plates.
- 1328 SCROCCA D., DOGLIONI C., RECANATI R., CHIARABBA C., GUERRINI M., FERRANTE V. & ANASTASIO M. (2006). -
1329 Caratterizzazione delle principali strutture sismogenetiche nell'offshore della Sicilia settentrionale. Abstracts
1330 GNGTS, Roma, 28-30 november 2006.
- 1331 SÉBRIER M., GHAFIRI A. & BLES J.-L. (1997). - Paleoseismicity in France: Fault trench studies in a region of moderate
1332 seismicity. - *J. Geodyn.*, **24**, 207-217.
- 1333 SELVAGGI G. (2006). - La Rete Integrata Nazionale GPS (RING) dell'INGV: un'infrastruttura aperta per la ricerca
1334 scientifica. X Conferenza ASITA, pp. 1749-1754, Bolzano.
- 1335 SERPELLONI E., ANZIDEI M., BALDI P., CASULA G. & GALVANI A. (2005). - Crustal velocity and strain-rate fields in
1336 Italy and surrounding regions: new results from the analysis of permanent and non-permanent GPS networks. -
1337 *Geophys. J. Int.*, **161**, 861-880.

- 1338 SERPELLONI E., CASULA G., GALVANI A., ANZIDEI M. & BALDI P. (2006). - Data analysis of permanent GPS networks in
1339 Italy and surrounding regions: application of a distributed processing approach. – *Ann. Geoph.*, **49**, 897-928.
- 1340 SERPELLONI E., VANNUCCI G., PONDRELLI S., ARGNANI A., CASULA G., ANZIDEI M., BALDI P., & GASPERINI P. (2007). -
1341 Kinematics of the western Africa-Eurasia plate boundary from local mechanisms and GPS data. - *Geophys. J.*
1342 *Int.*, **169**, 1180-1200.
- 1343 SHEMENDA A.I. (1992). - Horizontal lithosphere compression and subduction: Constraints provided by physical
1344 modelling. - *J. Geophys. Res.*, **97**, 11097–11116.
- 1345 SHEN Z.-K., JACKSON D. & GE B. (1996). - Crustal deformation across and beyond the Los Angeles basin from geodetic
1346 measurements. - *J. Geophys. Res.*, **101**, 27957-27980.
- 1347 SHEN Z.-K., JACKSON D.D. & KAGAN Y.Y. (2007). - Implications of geodetic strain rate for future earthquakes, with a
1348 five-year forecast of M5 earthquakes in southern California. – *Seismol. Res. Lett.*, **78**, 116-120.
- 1349 SOURIAU A. (1984). – Geoid anomalies over Gorringer Ridge, North Atlantic Ocean. – *Earth Planet. Sc. Lett.*, **68**, 101-
1350 114.
- 1351 SPERANZA F., VILLA I.M., SAGNOTTI L., FLORINDO F., COSENTINO D., CIPOLLARI P. & MATTEI M. (2002). - Age of the
1352 Corsica–Sardinia rotation and Liguro–Provençal basin spreading: new paleomagnetic and Ar/Ar evidence.
1353 *Tectonophysics*, **347**, 231–251.
- 1354 STICH D., AMMON C.J. & MORALES J. (2003). - Moment tensor solutions for small and moderate earthquakes in the
1355 Ibero–Maghreb region. - *J. Geophys. Res.*, **108**, 2148, doi:10.1029/2002JB002057.
- 1356 STICH D., MANCILLA F., BAUMONT D. & MORALES J. (2005). - Source analysis of the Mw 6.3 2004 Al Hoceima
1357 earthquake (Morocco) using regional apparent source time functions. – *J. Geophys. Res.*, **110**, B06306,
1358 doi:10.1029/2004/B003366.
- 1359 STICH D., SERPELLONI E., MANCILLA F.D. & MORALES J. (2006). - Kinematics of the Iberia–Maghreb plate contact from
1360 seismic moment tensors and GPS observations. - *Tectonophysics*, **426**, 295-317.
- 1361 STRZERZYNSKI P., DÉVERCHÈRE J., CATTANEO A., DOMZIG A., YELLES K., MERCIER DE LEPINAY B., BABONNEAU N. &
1362 BOUDIAF A. (2010). – Tectonic inheritance and Pliocene–Pleistocene inversion of the Algerian margin around
1363 Algiers: Insights from multibeam and seismic reflection data. – *Tectonics*, **29**, TC2008,
1364 doi:10.1029/2009TC002547.
- 1365 SUE C., THOUVENOT F., FRECHET J. & TRICART P. (1999). - Widespread extension in the core of the Western Alps
1366 revealed by earthquake analysis. - *J. Geophys. Res.*, **104**, 25611–25622.
- 1367 SUE C. & TRICART P. (2003). - Neogene to current normal faulting in the inner Western Alps: a major evolution of the
1368 late alpine tectonics. *Tectonics*, **22**, 1050, doi:10.1029/2002TC001426.
- 1369 TAHAYT A., MOURABIT T., RIGO A., FEIGL K.L., FADIL A., MCCLUSKY S., REILINGER R., SERROUKH M., OUAZZANI-
1370 TOUHAMI A., SARI D.B. & VERNANT P. (2008). - Mouvements actuels des blocs tectoniques dans l’arc Bético-
1371 Rifain à partir des mesures GPS entre 1999 et 2005. - *C. R. Geoscience*, **340**, 400–413.
- 1372 TENG L.S., LEE C.T., TSAI Y.B. & HSIAO L.Y. (2000). - Slab breakoff as a mechanism for flipping of subduction
1373 polarity in Taiwan. - *Geology*, **28**, 155-158.
- 1374 TESAURO M., KABAN M.K. & CLOETINGH S. (2008). - EuCRUST-07: a new reference model for the European crust. -
1375 *Geophys. Res. Lett.*, **35**, L05313, doi:10.1029/2007GL032244.
- 1376 THOMAS M.F.H., BODIN S., REDFERN J. & IRVING D.H.B. (2010). - A constrained Africa-craton source for the Cenozoic
1377 Numidian Flysch: implications for the palaeogeography of the western Mediterranean basin. - *Earth-Science*
1378 *Reviews*, **101**, 1-23.
- 1379 TORNE M., FERNÁNDEZ M., COMAS M.C. & SOTO J.I. (2000). – Lithospheric structure beneath the Alboran Basin:
1380 Results from three-dimensional gravity modeling and tectonic relevance. - *J. Geophys. Res.*, **105**, 3209-3228.
- 1381 TOTH J. & GURNIS M. (1998). - Dynamics of subduction initiation at preexisting fault zones. - *J. Geophys. Res.*, **103**,
1382 18053–18067, doi:10.1029/98JB01076.
- 1383 TYSON A.R., MOROZOVA E.A., KARLSTROM K.E., CHAMBERLAIN K.R., SMITHSON S.B., DUEKER K.G. & FOSTER C.T.
1384 (2002). - Proterozoic Farwell Mountain–Lester Mountain suture zone, northern Colorado: Subduction flip and
1385 progressive assembly of arcs. - *Geology*, **30**, 943-946.
- 1386 VAN DER VOO R., SPAKMAN W. & BIJWAARD H. (1999). - Mesozoic subducted slabs under Siberia. - *Nature*, **397**, 246-
1387 249.
- 1388 VANNUCCI G., PONDRELLI S., ARGNANI A., MORELLI A., GASPERINI P. & BOSCHI E. (2004). - An atlas of Mediterranean
1389 seismicity. *Ann. Geophys.*, **47**, 247-306.
- 1390 VIGNAROLI G., FACCENNA C., JOLIVET L., PIROMALLO C. & ROSSETTI F. (2008). – Subduction polarity reversal at the
1391 junction between the Western Alps and the Northern Apennines, Italy. - *Tectonophysics*, **450**, 34-50.
- 1392 VIGNAROLI G., ROSSETTI F., THEYE T. & FACCENNA C. (2008). - Styles and regimes of orogenic thickening in the
1393 Peloritani Mountains (Sicily Italy): new constraints on the tectono-metamorphic evolution of the Apennine belt. -
1394 *Geol. Mag.*, **145**, 552-569.
- 1395 VIGNAROLI G., FACCENNA C., ROSSETTI F. & JOLIVET L. (2009). - Insights from the Apennines metamorphic complexes
1396 and their bearing on the kinematics evolution of the orogen. *Geol. Soc., London, Sp. Publ.*, **311**, 235-256.
- 1397 WHITE D.J., LUCAS S.B., BLEEKER W., HAJNAL Z., LEWRY J.F. & ZWANZIG H.V. (2002). - Suture-zone geometry along
1398 an irregular Paleoproterozoic margin: the Superior boundary zone, Manitoba, Canada. - *Geology*, **30**, 735-738.

1399 WILLIAMS S.D.P., BOCK Y., FANG P., JAMASON P., NIKOLAIDIS R.M., PRAWIRODIRDJO L., MILLER M. & JOHNSON D.J.
1400 (2004). - Error analysis of continuous GPS position time series. - *J. Geophys. Res.*, **109**, B03412,
1401 doi:10.1029/2003JB002741.
1402 WILSON J.T. (1963). - Evidence from islands on the spreading of ocean floors. - *Nature*, **197**, 536-538.
1403 WORTEL M.J.R. & SPAKMAN W. (2000). - Subduction and slab detachment in the Mediterranean-Carpathian region. -
1404 *Science*, **290**, 1910-1917.
1405 YELLES A., DOMZIG A., DÉVERCHÈRE J., BRACÈNE R., MERCIER DE LÉPINAY B., STRZERZYNSKI P., BERTRAND G.,
1406 BOUDIAF A., WINTER T., KHERROUBI A., LE ROY P. & DJELLIT H. (2009). - Plio-Quaternary reactivation of the
1407 Neogene margin off NW Algiers, Algeria: the Khayr al Din bank. - *Tectonophysics*, **475**, 98-116.
1408 ZITELLINI N., GRÀCIA E., MATIAS L., TERRINHA P., ABREAU M.A., DE ALTERIIS G., HENRIET J.P., DAÑOBEITIA J.J.,
1409 MASSON D.G., MULDER T., RAMELLA R., SOMOZA L. & DIEZ S. (2009). - The quest for the Africa-Eurasia plate
1410 boundary west of the Strait of Gibraltar. *Earth Planet. Sc. Lett.*, **280**, 13-50.
1411 ZOBACK M.L. (1992). - First- and second-order patterns of stress in the lithosphere: The World Stress Map project. - *J.*
1412 *Geophys. Res.*, **97**, 703-11, 728.

1413 **FIGURE CAPTIONS**

1414 **Figure 1. (a)** Tectonic setting of the western Mediterranean area [Cadet and Funicciello, 2004]. **(b)**
1415 Moho depth (below sea level) in the western Mediterranean area [Tesauro *et al.*, 2008].
1416 Numbers are Moho depth in km. Abbreviations are as follows: A, Apennines; AB, Alboran
1417 Basin; AP, Adriatic Promontory; BC, Betic Cordillera; BS, Black Sea; CM, Cantabrian Mts;
1418 D, Dinarides; FB, Focvani Basin; MC, Massif Central; P, Pyrenees; PB, Pannonian Basin; TS,
1419 Tyrrhenian Sea; URG, Upper Rhine Graben; VT, Valencia Trough.

1420
1421
1422 **Figure 2.** Schematic tectonic evolution of the western Mediterranean subduction zone between
1423 Nubia and Eurasia since 35 Ma [Faccenna *et al.*, 2004].

1424
1425
1426 **Figure 3.** Seismic cross-sections across the Liguro-Provençal and Algerian margins. **(a)** High-
1427 resolution MDJS43 seismic reflection profile acquired across the eastern Algerian margin,
1428 showing anticlinal deformations and inferred S-dipping, N-verging thrusts [Kherroubi *et al.*,
1429 2009]. **(b)** High-resolution A (Maradja cruise) seismic reflection profile acquired across the
1430 central Algerian margin, showing anticlinal deformations and inferred S-dipping, N-verging
1431 thrusts [Domzig *et al.*, 2006]. S = salt. **(c)** High-resolution MA31 seismic reflection profile
1432 acquired across the Liguro-Provençal basin, showing a NE-dipping reflection dubiously
1433 interpreted as a late Pliocene-Quaternary S-verging thrust inverting the basin margin since
1434 about 3.5 Ma [Bigot-Cormier *et al.*, 2004]. S = salt.

1435
1436
1437 **Figure 4.** High-penetration seismic profile across the south-Tyrrhenian margin [Pepe *et al.*, 2005].
1438 See the cross-section track in Fig. 3. The hypocenter of the 2002 “Palermo” earthquake ($M_w =$
1439 5.6, compressional fault plane solution) is approximately located on a N-dipping, S-verging
1440 reverse fault below the crystalline thrust sheet (KCU). The yellow bar is the error bar for the
1441 hypocenter depth.

1442
1443
1444 **Figure 5. (a)** Crustal (depth ≤ 35 km) earthquakes occurred between 1962 and 2009 in the western
1445 Mediterranean region. Data are from the ISC Bulletin (<http://www.isc.ac.uk/>) and include
1446 earthquakes with magnitude ≥ 4 . **(b)** Same as (a) for intermediate and deep (depth > 35 km)
1447 earthquakes. **(c)** Epicentral map of $M \geq 4$ earthquakes occurred between 1900 and 1961 (data
1448 are from the EUROSEISMOS catalog available online at http://storing.ingv.it/es_web/).

1449
1450
1451 **Figure 6.** Maps of moment tensor solutions for crustal, $M \geq 4.5$ earthquakes. **(a)** Data are from the
1452 Harvard CMT catalog (1976-2009, <http://www.globalcmt.org/CMTsearch.html>). Grey
1453 background solutions indicate data also shown in (b). **(b)** Data are from the RCMT catalog
1454 (1997-2004, http://www.bo.ingv.it/RCMT/yearly_files.html). Red = normal faulting, blue =
1455 thrust faulting, green = strike-slip faulting, and black = unknown stress regime (see text for
1456 details). **(c)** Polar plots of P- and T-axes for earthquakes grouped in sectors of significant
1457 seismic relevance (red = CMT and blue = RCMT). Full and empty dots correspond to P- and
1458 T-axes, respectively. Dashed line indicates the Adria lithosphere according to Chiarabba *et al.*
1459 [2005]. For the 1997-2004 time interval, P- and T-axes values included in (c) are taken from
1460 the RCMT catalog, whereas data pertaining to the grey background solutions plotted in (a) are
1461 not considered.

1462

1463
1464
1465
1466
1467
1468
1469
1470
1471
1472
1473
1474
1475
1476
1477
1478
1479
1480
1481
1482
1483
1484
1485
1486
1487
1488
1489
1490
1491
1492
1493
1494
1495
1496
1497
1498
1499
1500
1501
1502
1503
1504

Figure 7. (a) Horizontal GPS velocities given with respect to a fixed Eurasian frame (see text). Red arrows show observed velocities, with 95% error ellipses; white arrows show the velocities predicted by the Nubia-Eurasia relative rotation pole; grey arrows show the interpolated velocity field, obtained from inversion of the horizontal velocity gradient field (see text). (b) Horizontal strain-rate field obtained from least-squares interpolation of the horizontal velocity field presented in (a). Red diverging arrows show extensional strain-rates, whereas blue converging arrows show contractional.

Figure 8. Velocity anomalies in the upper mantle below the western Mediterranean area after the tomographic model of Piromallo and Morelli [2003]. P-velocity perturbation is displayed with respect to reference model *sp6* [Morelli and Dziewonski, 1993].

Figure 9. Three-dimensional tomographic-topographic model (tomography after Piromallo and Morelli, 2003) of the western Mediterranean region. The isosurface encloses a volume characterized by P-wave velocity anomalies larger than 0.6% relative to the reference model. Hypothetical future segments of the Nubia-Eurasia convergent boundary (indicated as incipient convergent boundary) are inferred from the original and previously-published evidence presented in this paper. Basin inversion has propagated in a scissor-like manner from the Alboran basin (c. 8 Ma) to the south-Tyrrhenian domain (younger than c. 2 Ma) following a similar propagation of the subduction cessation, i.e., older to the west and younger to the east (Table 1). Color code of the incipient convergent boundary indicates progressively younger (lighter color) inversion or compression from west to east (see age numerical indications for the onset of compression-inversion). The possibility of a new convergent boundary in the Liguro-Provençal region is still debated (see the text). Dashed segments of the incipient boundary are between Tunisia and Sicily, where no oceanic crust occurs and the occurrence of a future convergent boundary is therefore unlikely, and in the southern Iberian margin, where basin inversion is not as advanced as in the opposite Algerian margin. The track of the former subduction zone (trench) can be inferred from relics of the Nubian slab to the east of Sicily (Calabrian arc) and in the Algerian inland.

Figure 10. Cartoon showing the proposed model of subduction inception. Subduction inception is influenced by friction along the plate interface and therefore by the size of the interface [Toth and Gurnis, 1998]. The lateral propagation, in a scissor-like fashion, of the new plate boundary may result less friction-resistant than other models of subduction inception where subduction is initiated all at once along longer segments of the new plate boundary. In the case of the western Mediterranean, the area of subduction inception corresponds with the Algerian margin [Strzeczynski *et al.*, 2010] and the propagation of subduction is toward the east. The Alboran basin is excluded by this process (subduction) for the substantial absence of oceanic crust.

Table 1. Tentative ages for slab window formation and onset of backarc compression in the western Mediterranean. These episodes are inferred from the available literature and help to understand the spatio-temporal evolution of the tectonic reorganization in the study area, i.e., from subduction cessation to backarc compression and inversion perhaps leading to subduction of former backarc basins. Proposed references are only a selection of the vast literature on the subject (see text).

slab window formation			backarc compression		
geographic location	age of slab window	Ref.	geographic location	age of backarc compression onset	Ref.
Oranie-Melilla (Morocco-Algeria)	~ 15 Ma	(1), (2)	Alboran margin	~ 8 Ma	(5), (6)
Nefza and Mogodos (Tunisia)	~ 10-8 Ma	(2), (3)	Algerian margin	~ 7-5 Ma	(7)
Prometeo and Ustica (S-Tyrrhenian)	~ 4 Ma	(2), (4)	Provençal margin	~ 3.5 Ma	(8)
			S-Tyrrhenian margin	younger than ~ 2 Ma	(9), (10)

(1) Coulon *et al.*, [2000]; (2) Faccenna *et al.*, [2004]; (3) Maury *et al.*, [2000]; (4) Faccenna *et al.*, [2005]; (5) Bourgois *et al.*, [1992]; (6) Comas *et al.*, [1999]; (7) Mauffret, [2007]; (8) Bigot-Cormier *et al.*, [2000]; (9) Goes *et al.*, [2004]; (10) Billi *et al.*, [2007].

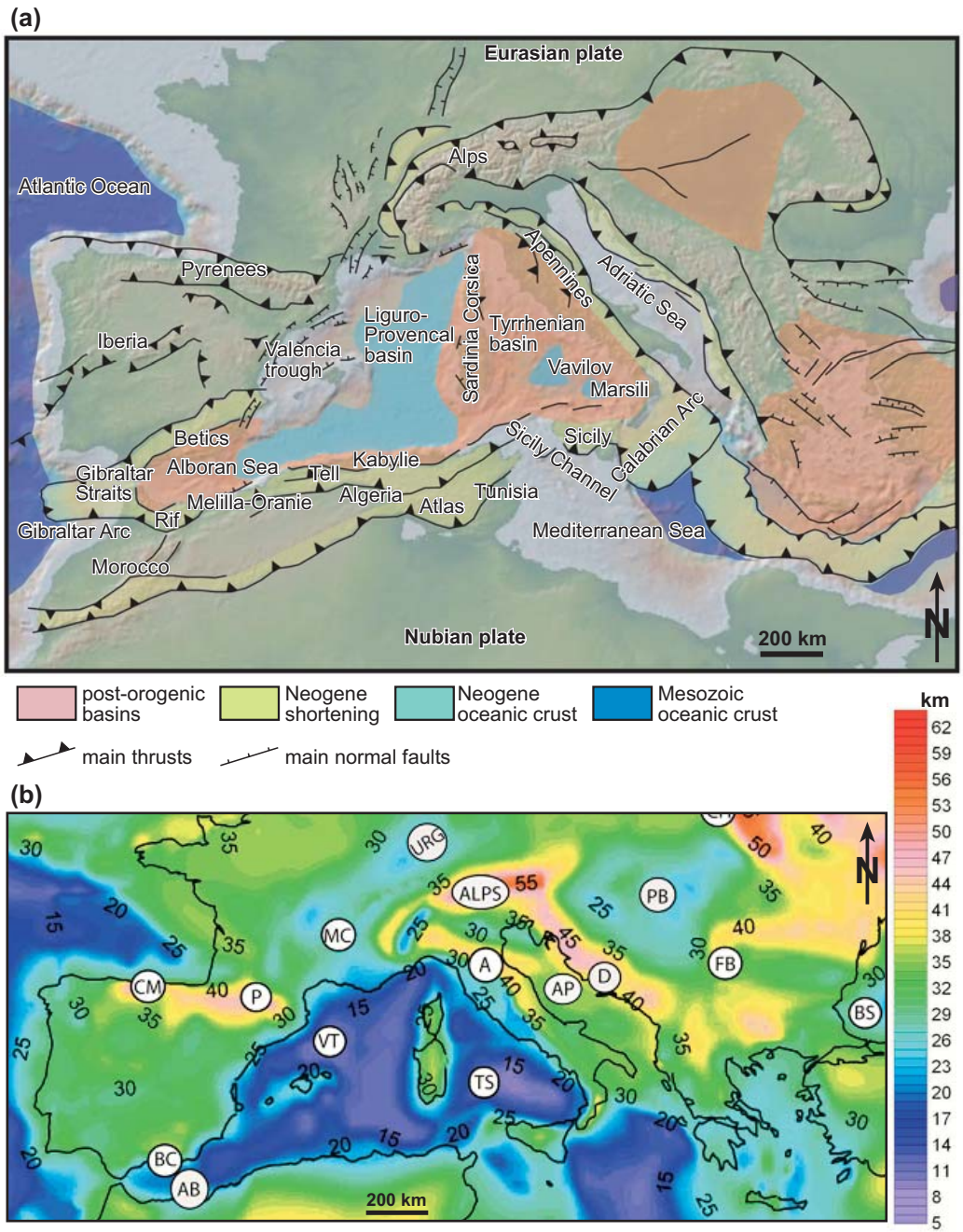


Figure 1

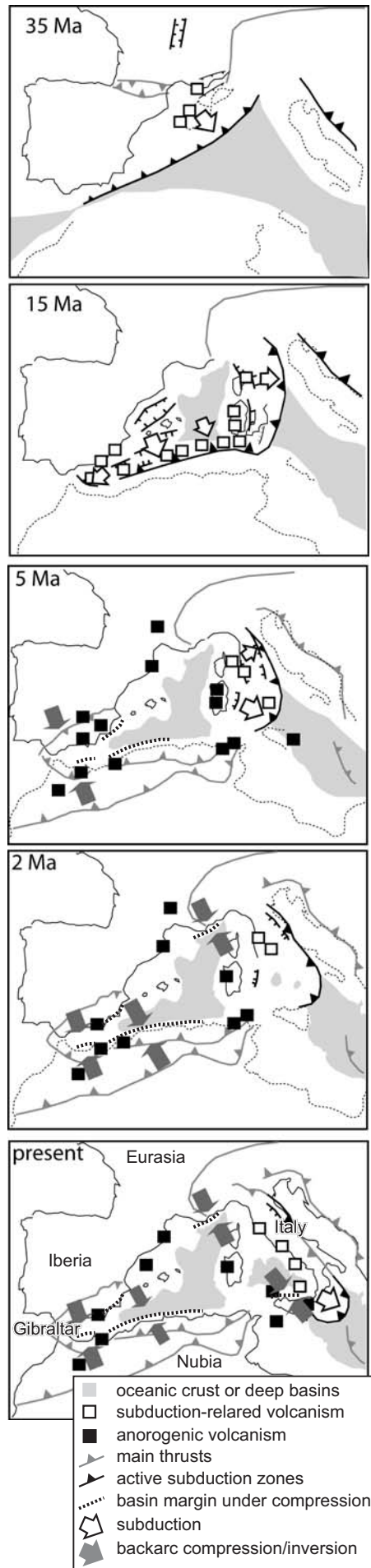


Figure 2

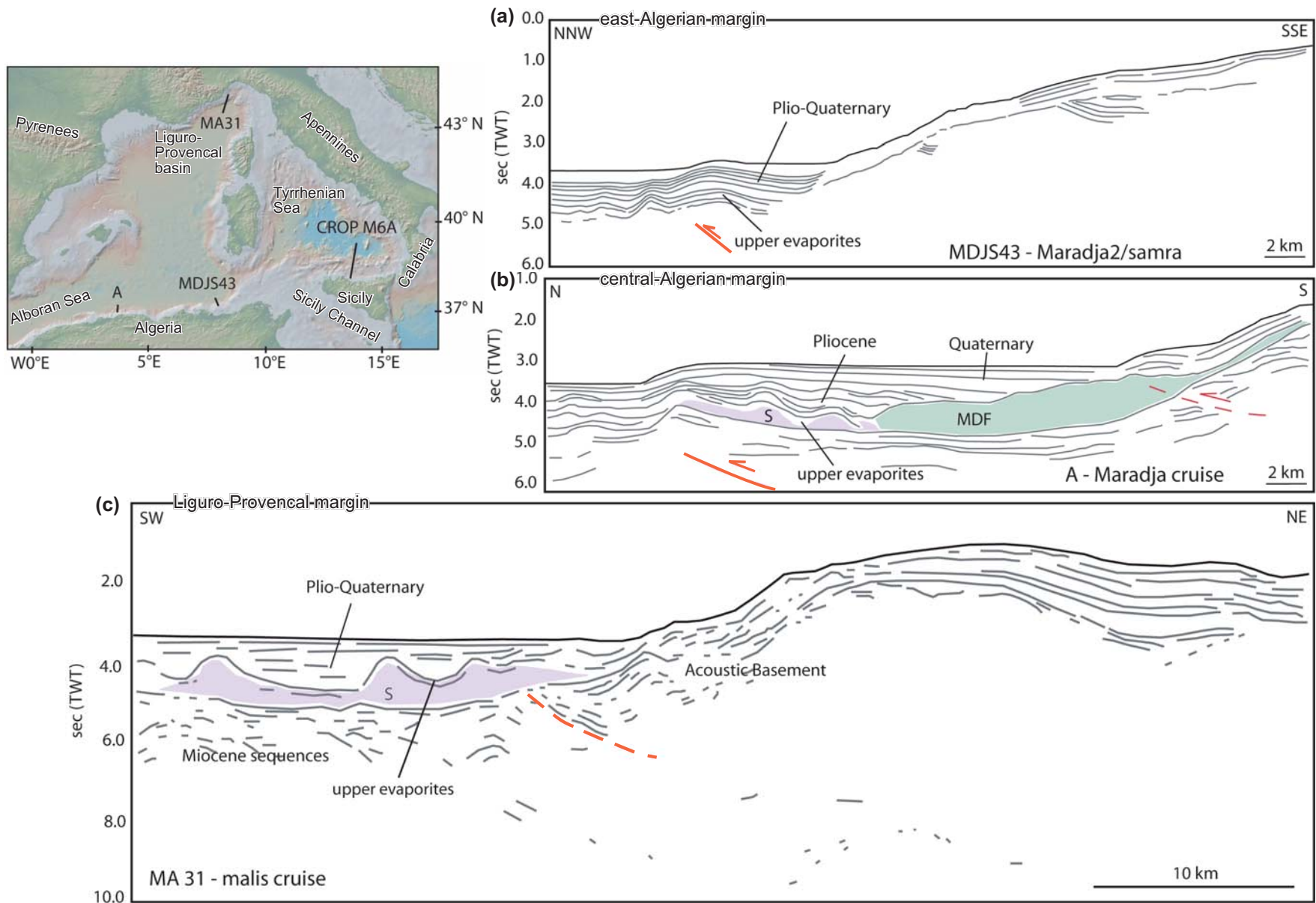


Figure 3

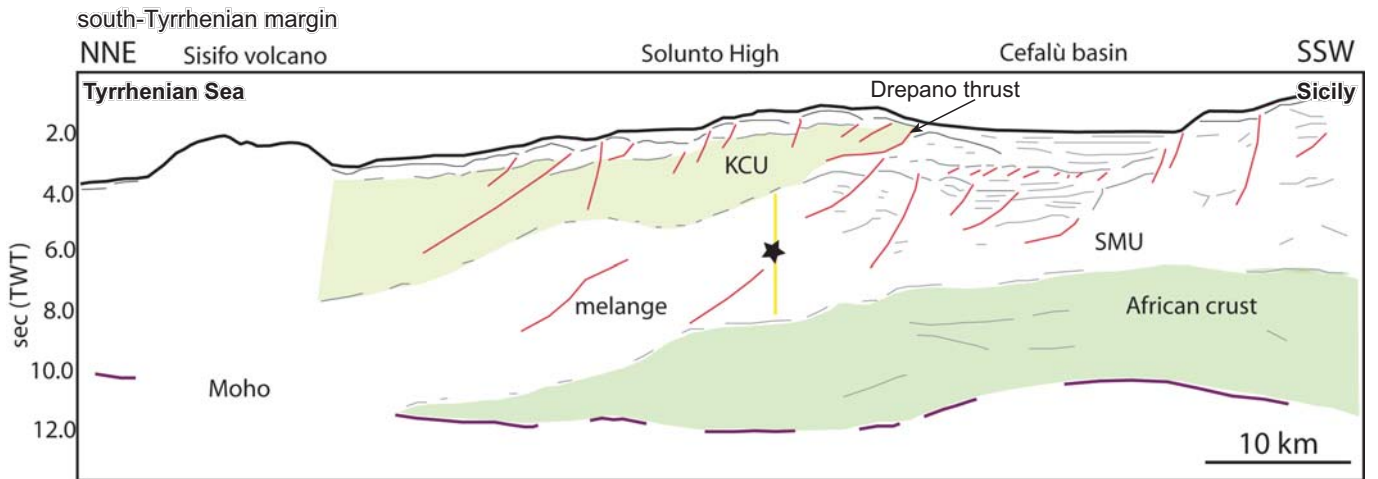


Figure 4

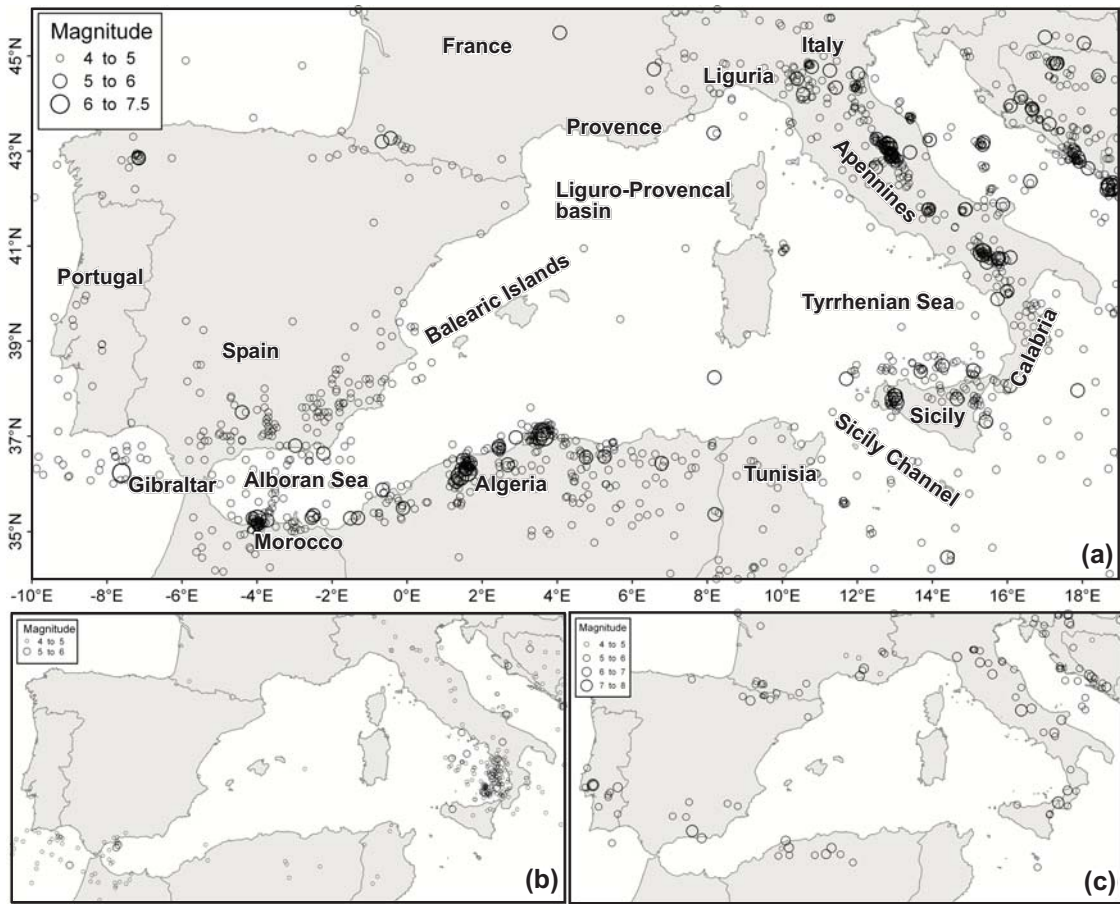


Figure 5

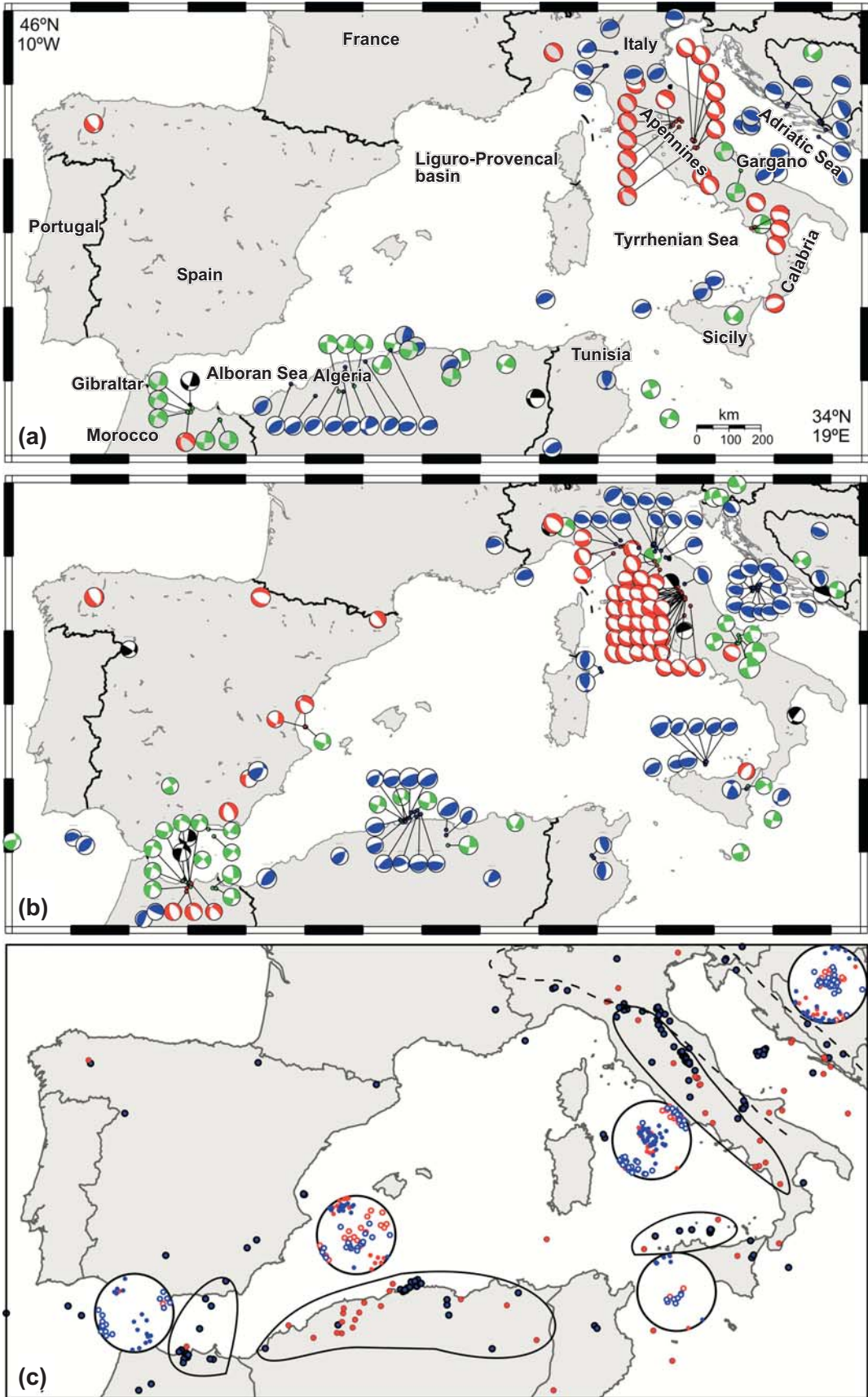


Figure 6

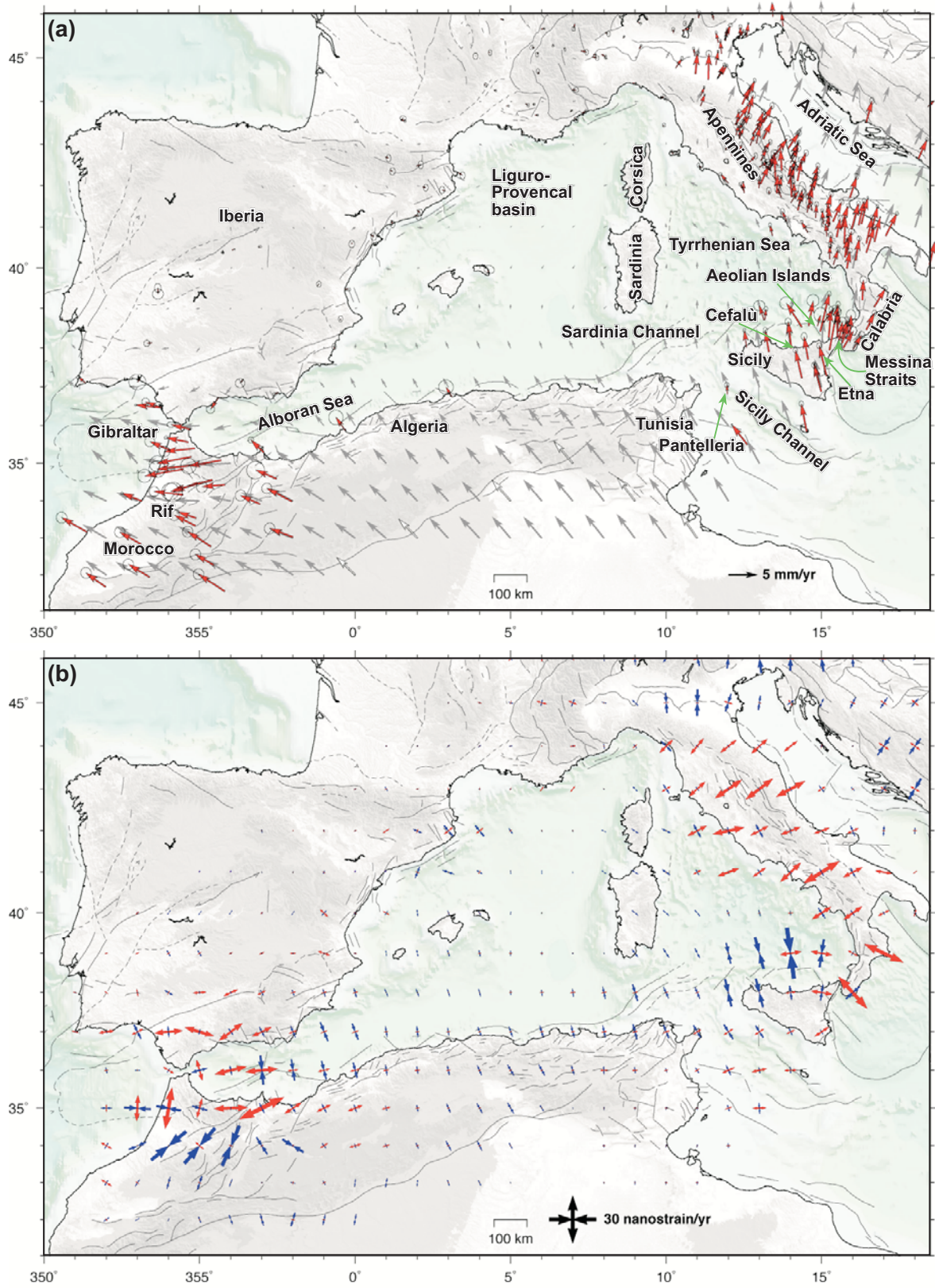


Figure 7

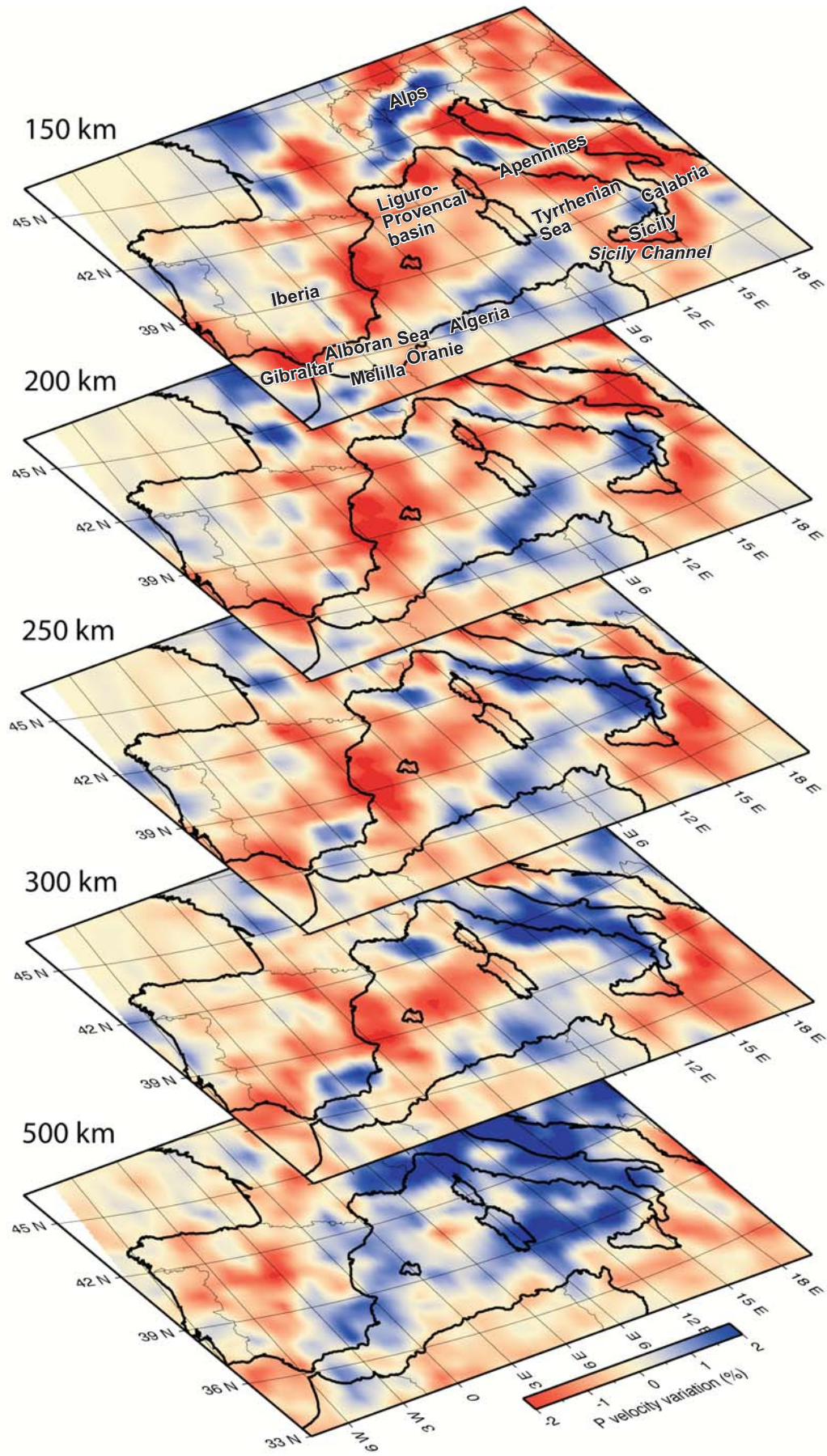


Figure 8

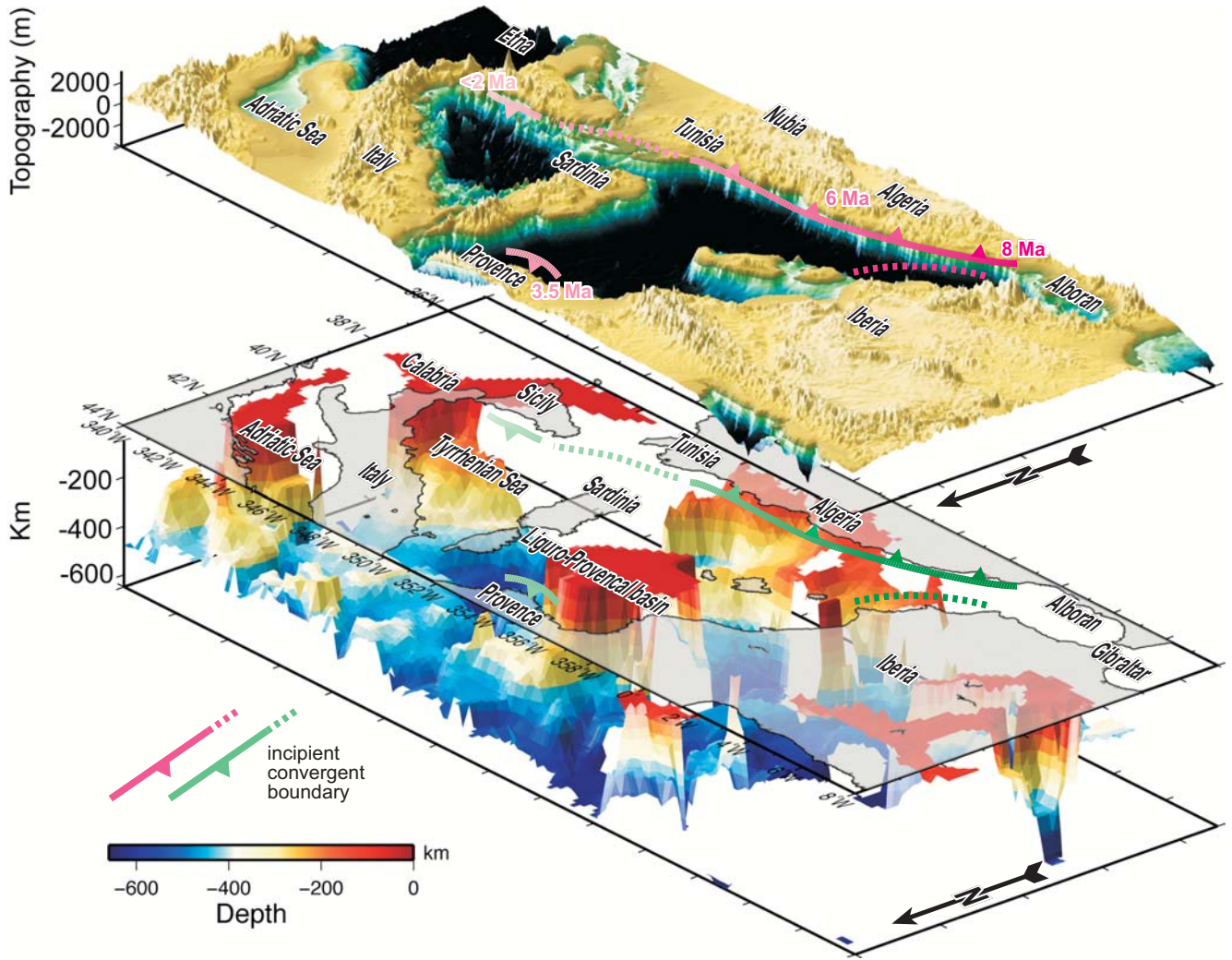


Figure 9

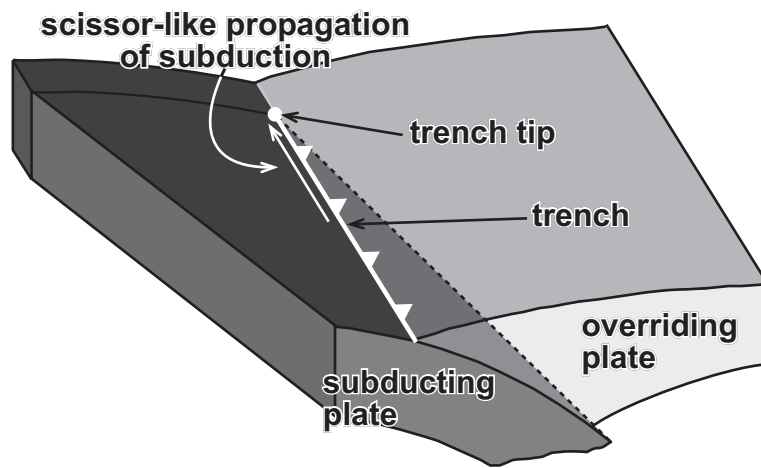


Figure 10